UNIVERSIDADE FEDERAL DE VIÇOSA

Intelligent UAV Systems: Payload Monitoring for Spraying and Collaborative Cargo Transport

Celso Oliveira Barcelos
Magister Scientiae

VIÇOSA - MINAS GERAIS
2025

CELSO OLIVEIRA BARCELOS

Intelligent UAV Systems: Payload Monitoring for Spraying and Collaborative Cargo Transport

Dissertation submitted to the Computer Science Graduate Program of the Universidade Federal de Viçosa in partial fulfillment of the requirements for the degree of *Magister Scientiae*.

Adviser: Alexandre Santos Brandao

Co-adviser: Daniel Ceferino Gandolfo

VIÇOSA - MINAS GERAIS
2025

Ficha catalográfica elaborada pela Biblioteca Central da Universidade Federal de Viçosa - Campus Viçosa

T

B242p
2025

Barcelos, Celso Oliveira, 1994-

Intelligent UAV systems: payload monitoring for spraying and collaborative cargo transport / Celso Oliveira Barcelos. – Viçosa, MG, 2025.

1 dissertação eletrônica (73 f.): il. (algumas color.).

Texto em inglês.

Inclui apêndice.

Orientador: Alexandre Santos Brandão.

Dissertação (mestrado) - Universidade Federal de Viçosa, Departamento de Informática, 2025.

Referências bibliográficas: f. 65-67.

DOI: https://doi.org/10.47328/ufvbbt.2025.433

Modo de acesso: World Wide Web.

1. Robótica. 2. Agricultura de precisão. 3. Armazenamento e transporte de carga. 4. Aeronáutica. I. Brandão, Alexandre Santos, 1982-. II. Universidade Federal de Viçosa. Departamento de Informática. Programa de Pós-Graduação em Ciência da Computação. III. Título.

CDD 22. ed. 629.892

Bibliotecário(a) responsável: Euzébio Luiz Pinto CRB-6/3317

CELSO OLIVEIRA BARCELOS

Intelligent UAV Systems: Payload Monitoring for Spraying and Collaborative Cargo Transport

Dissertation submitted to the Computer Science Graduate Program of the Universidade Federal de Viçosa in partial fulfillment of the requirements for the degree of *Magister Scientiae*.

APPROVED: March 26, 2025.

Assent:

Celso Oliveira Barcelos
Author

Alexandre Santos Brandao
Adviser

ACKNOWLEDGMENTS

Pessoalmente, considero esta uma das partes mais importantes em cada fase de nossas vidas, saber reconhecer e agradecer pelas experiências, amizades, risadas ao longo de nossas vidas. É o momento de desacelerar, refletir, e demonstrar gratidão com aqueles que sempre nos dão forças para seguir em frente, seja nos bons momento, mas principalmente nos difíceis.

Agradeço primeiramente a Deus, principalmente pela segunda chance que me foi dada, a partir do meu acidente em 2015 sou outra pessoa dada as consequências e os aprendizados pelos quais enfrentei. Apesar do grande susto que causei aos meus familiares e amigos, eu não teria chegado onde cheguei sem esse tranco que a vida me deu. A partir deste episódio, carrego comigo que apesar dos “tombos” que a vida nos dá, sempre temos o que aprender e devemos focar nossas forças no que deve ser feito para levantarmos ainda mais fortes.

Em segundo lugar, quero expressar minha gratidão aos meus pais, Afonso e dona Tita, pois sou muito grato pelos ensinamentos que me proporcionaram, especialmente sobre humildade e caráter. Mesmo com todas as dificuldades enfrentadas na roça, sempre tivemos bons exemplos dentro de casa. Espero, com fervor, honrá-los da maneira que merecem!

Agradeço de coração à minha irmã Lúcia e meus irmãos Silvio e Vitor pelo carinho e apoio constante que sempre me ofereceram. À minha namorada Jaqueliny, meu muito obrigado por ter me encorajado e dado forças durante minha trajetória na UFV, além de ter cuidado de mim durante minha recuperação pós-acidente. Sou grato também ao meu padrinho Verinho, pois sem seu valioso incentivo, eu não teria chegado tão longe. Um agradecimento especial aos meus amigos da ELT 18 e agora do mestrado: Hiago, Wérikson, Mateus careca e Anaílson. Foram muitos trabalhos e estudos em grupo, mas também muitas risadas nos arredores da universidade. Ao Hiago em especial, foram muitos choops no Murato e no Registrada ao longo do mestrado, obrigado por ser meu grande amigo de desabafo, mas também de boas resenhas, como você sempre dizia: “Um ambiente de bullying, não me cabe.”

Não posso esquecer do Leo, vulgo Leozinho do drone ou Leodinho, segundo nossos amigos de INAUT (Daniel Gandolfo, Fernando, Christian, Kleber, Pedro, Jeysson, Luiz, Bryan e Daniel). Mais que um amigo, considero como um irmão que ganhei na universidade. Um amigo de projetos que tive a oportunidade de aprender inúmeras coisas com sua experiência e paciência em ensinar. Sou eternamente grato pela grande parceria nos vários trabalhos em dupla, às conquistas e raivas que passamos quando as coisas não caminhavam bem, quando os robôs iam pro teto ou paredes e precisavam ser segurados na unha, pelo drone quebrado que nos rendeu algumas de insônia, sem contar os perrengues vivenciados durante nosso intercâmbio na Argentina, mas que de onde não podemos esquecer dos bueníssimos assados.

Também não posso deixar de lembrar dos meus parceiros e amigos do BDP e NERo, em especial ao Sacola, Joãozinho cabeleira, vulgo “fogo no matinho”, Gabriel tanguinha, Felipe, Gabriel MMA, e Guilherme Chico. Foram muitas experiências divertidas dentro do laboratório assim como vários aprendizados que contribuíram para meu desenvolvimento profissional enquanto estudante.

Gostaria de dedicar algumas palavras ao pessoal do tecnoPARQ, que me recebeu com muito carinho desde minha chegada em maio de 2024, para atuar nos laboratórios makers. Agradeço especialmente à Diretora e professora Adriana, cujo apoio foi fundamental para que eu pudesse realizar minhas atividades com confiança. Meus sinceros agradecimentos também vão para as coordenadoras Jucélia e Francylara, carinhosamente referida como Fran, pela orientação em relação aos meus deveres no parque, sinto-me honrado por ter conhecido cada uma delas, pois aprendi e evoluí significativamente como profissional. Aos meus estagiários; Lucas, Pablo Valentim, Pedro, Estêvão, Pablo Mendes e Altair, saibam que aprendi muito mais com vocês do que vocês comigo. Por fim, tomo a liberdade de agradecer aos demais funcionários do parque em nome da Carol, Claudinei, Marcus Vinicius, Vinícius, Mauro e seu irmão Luizinho, Fred e Maria Célia. Meu muito obrigado a todos!

Não menos importante, preciso agradecer aos professores do DPI, Michel, Ricardo, Arroyo, Willian da secretaria do PPGCC, e demais funcionários. Falando em professores, muito obrigado a querida professora (que hoje tenho mais como amiga) Geice, passamos por alguns perrengues juntos

até botar a nossa disciplina de lato sensu rodando. Em especial ao meu professor, orientador e grande amigo Alexandre Brandão, famoso Timóteo, por acreditar em minhas habilidades assim que entrei no BDP em 2018, mesmo quando eu duvidava não ser capaz. Pela confiança empregada em mim, pelas orientações e ensinamentos desde então. Seus conhecimentos foram e continuarão sendo decisivos na minha formação acadêmica. Para você, deixo a famosa frase icônica: “Se você gosta disso, saiba que eu gosto 33 vezes mais...”

Por fim, sou grato à Universidade Federal de Viçosa como um todo, sem ela eu não teria tido a oportunidade de conhecer pessoas tão incríveis que contribuíram direta ou indiretamente para minha formação como Engenheiro Eletricista, e agora como mestre em Ciências da Computação. Serei eternamente agradecido por poder carregar comigo o selo UFV de qualidade!
E para terminar, quero encerrar meus agradecimentos à Coordenação de Aperfeiçoamento de Pessoal de Nível Superior – Brasil (CAPES) – Finance Code 001, que através de seu financiamento, tive a oportunidade de finalizar este curso de pós-graduação.

This work has been sponsored by the following Brazilian research agencies: Coordination for the Improvement of Higher Education Personnel (CAPES; Financing code 001), Minas Gerais State Foundation for Research Aid (FAPEMIG) and National Council of Scientific and Technological Development (CNPq).

"Parte da jornada,
é o fim..."

(Tony Stark).

ABSTRACT

BARCELOS, Celso Oliveira, M.Sc., Universidade Federal de Viçosa, March, 2025. **Intelligent UAV Systems: Payload Monitoring for Spraying and Collaborative Cargo Transport**. Adviser: Alexandre Santos Brandao. Co-adviser: Daniel Ceferino Gandolfo.

The use of unmanned aerial vehicles (UAVs) has been expanding rapidly, bringing innovations to various areas, such as precision agriculture and logistics. This dissertation investigates the integration of payload sensors into UAVs to improve agricultural spraying tasks and collaborative cargo transportation. Initially, a real-time payload monitoring system is proposed, which allows the UAV to adjust the application of agricultural inputs according to the variation in the weight of the spray tank. This mechanism avoids waste and improves the efficiency of the operation. In addition, an intelligent navigation system was developed that monitors the tank level and commands automatic return to base when necessary. To validate the proposal, experiments were conducted in controlled environments, demonstrating the system's effectiveness in controlling the distribution of inputs. In addition to agricultural applications, this research addresses the cooperative transportation of cargo by UAVs and unmanned ground vehicles (UGVs). An aerial transportation system was developed using a UAV equipped with an electromagnet suspended from a cable, making it possible to lift and move loads to overcome obstacles in the path of a UGV. Experimental tests have shown that the proposed approach is viable for applications such as urban deliveries, operations in remote areas and logistical support in disaster zones. The results obtained show that the integration of cargo sensors with intelligent control strategies promotes a significant improvement in UAV performance in various operational scenarios. This improvement is mainly due to the systems' ability to provide real-time information on the weight carried, allowing the UAV to make more precise autonomous decisions. This makes it possible to identify the ideal time to return to base for refuelling or to end the spraying mission, reducing waste and optimizing the use of inputs. In addition, there is more efficient management of energy consumption and flight time, based on the actual load carried. Another important advance is the automation of the load coupling and uncoupling processes, increasing agility in logistics missions and reducing the need for human intervention. These functionalities together result in safer, efficient and sustainable operations. Thus, the contributions of this work represent a relevant advance in the state of the art of UAV application in precision agriculture and autonomous cargo transportation.

Keywords: Precision Agriculture; Path following; Load Transportation; Multi-robot Systems; Cable-suspended cargo; UAV-UGV Cooperation

RESUMO

BARCELOS, Celso Oliveira, M.Sc., Universidade Federal de Viçosa, março de 2025. **Sistemas de UAV inteligentes: Monitoramento da Carga Útil para Pulverização e Transporte Colaborativo de Carga**. Orientador: Alexandre Santos Brandao. Coorientador: Daniel Ceferino Gandolfo.

O uso de veículos aéreos não tripulados (VANTs) tem se expandido rapidamente, trazendo inovações para diversas áreas, como agricultura de precisão e logística. Esta dissertação investiga a integração de sensores de carga em VANTs para aprimorar tarefas de pulverização agrícola e transporte colaborativo de cargas. Inicialmente, propõe-se um sistema de monitoramento de carga útil em tempo real, que permite ao VANT ajustar a aplicação de insumos agrícolas conforme a variação do peso do tanque de pulverização. Esse mecanismo evita desperdícios e melhora a eficiência da operação. Além disso, desenvolveu-se um sistema de navegação inteligente que monitora o nível do reservatório e comanda o retorno automático à base quando necessário. Para validar a proposta, foram conduzidos experimentos em ambientes controlados, demonstrando a eficácia do sistema no controle da distribuição dos insumos. Além da aplicação na agricultura, esta pesquisa aborda o transporte cooperativo de cargas por VANTs e veículos terrestres não tripulados (VTNTs). Um sistema de transporte aéreo foi desenvolvido utilizando um VANT equipado com um eletroímã suspenso por um cabo, possibilitando o levantamento e deslocamento de cargas para superar obstáculos no trajeto de um VTNT. Os testes experimentais demonstraram que a abordagem proposta é viável para aplicações como entregas urbanas, operações em áreas remotas e suporte logístico em zonas de desastre. Os resultados obtidos demonstram que a integração de sensores de carga com estratégias de controle inteligente promove uma melhora significativa no desempenho dos VANTs em diversos cenários operacionais. Essa melhoria se deve, principalmente, à capacidade dos sistemas em fornecer informações em tempo real sobre o peso transportado, permitindo que o VANT tome decisões autônomas mais precisas. Com isso, é possível identificar o momento ideal para retornar à base para reabastecimento ou encerrar a missão de pulverização, reduzindo desperdícios e otimizando o uso de insumos. Além disso, há uma gestão mais eficiente do consumo de energia e do tempo de voo, com base na carga real transportada. Outro avanço relevante é a automatização dos processos de acoplamento e desacoplamento de cargas, aumentando a agilidade em missões logísticas e reduz a necessidade de intervenções humanas. Essas funcionalidades, em conjunto, resultam em operações mais seguras, eficientes e

sustentáveis. Assim, as contribuições deste trabalho representam um avanço relevante no estado da arte da aplicação de VANTs na agricultura de precisão e no transporte autônomo de cargas.

Palavras-chave: Agricultura de Precisão; Seguimento de Caminho; Transporte de Cargas; Sistemas Multi-robôs; Carga suspensa por cabos; Cooperação UAV-UGV

List of Figures

List of Tables

Contents

1 Introduction

Unmanned Aerial Vehicles (UAVs) have gained significant attention in recent years for their versatility in various applications, including aerial surveillance, mapping, and agricultural monitoring. Among these applications, UAV-based cargo transportation has emerged as a promising area of research, particularly in scenarios where traditional ground-based transportation is impractical, inefficient or unsafe. The ability of UAVs to transport payloads over difficult terrain, disaster zones, or remote agricultural fields makes them an attractive alternative to conventional logistics and delivery methods UAVs can transport payloads using two primary approaches: (i) attaching the payload directly to their rigid body via mechanical, electromagnetic, or robotic grippers (CHEN et al., 2019; FIAZ; TOUMI; SHAMMA, 2017), or (ii) suspending the payload using cables, which preserves the UAV's maneuverability and enables flexible handling of various types of loads (SARKISOV et al., 2019; JIMÉNEZ-CANO et al., 2022; LOPEZ; MARTINEZ-CARRANZA, 2022).

The first technical involves attaching the payload directly to the UAV's rigid body via mechanical, electromagnetic, or robotic grippers (CHEN et al., 2019; FIAZ; TOUMI; SHAMMA, 2017) as shown in Figure 1. This method provides a stable attachment but can significantly affect the UAV's aerodynamics and maneuverability. The second approach suspends the payload using cables, preserving the UAV's agility while allowing for greater flexibility in handling various types of loads (SARKISOV et al., 2019; JIMÉNEZ-CANO et al., 2022; LOPEZ; MARTINEZ-CARRANZA, 2022). This type of approach is illustrated in Figure 2, where two strategies for carrying the load are shown, involving the number of UAVs used during the task. However, cable-suspended payloads introduce complex dynamic behaviors that require sophisticated control strategies to mitigate oscillations and ensure stable flight.

(a) Medical kit seizure maneuver presented in (UBELLACKER et al., 2024).

(b) The UAV resting on the gripper takes off and picks up the payload in blue presented in (KREMER et al., 2023).

Figure 1 – Experimental examples of aerial pick-and-place application using grippers.

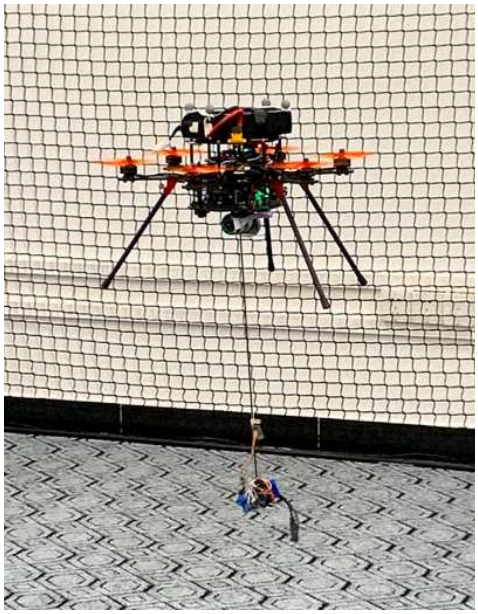

(a) Transport by single UAV, extracted of (HUANG et al., 2023).

(b) Transport by mult-robot UAV formation, presented in (LI; GE; LOIANNO, 2021).

Figure 2 – Load transportation task carrying a payload via suspended-cables.

The nature of the payload itself introduces additional challenges. Solid payloads, such as packages in logistics operations, have relatively predictable weight and center of mass, making them easier to model and control during transport (KOTARU; WU; SREENATH, 2018). Liquid payloads, such as pesticides and fertilizers, pose greater challenges due to fluid movement within the container, which can shift the center of mass dynamically and affect flight stability (TANG; WÜEST; KUMAR, 2018). Additionally, payloads with variable weight, such as pesticide tanks that gradually empty during flight, require real-time weight monitoring to adjust flight parameters accordingly and ensure efficiency in mission execution (MOGILI; DEEPAK, 2018).

According to Villa, Brandao e Sarcinelli-Filho (2020), a UAV carrying a cargo changes its dynamic model, as the added mass alters its flight characteristics and energy consumption. Increased thrust requirements lead to higher energy expenditure, reducing flight endurance and operational range. Consequently, cooperative transportation strategies have been proposed, where multiple UAVs work together to distribute the load, reducing the burden on individual aircraft and increasing efficiency (CARDONA; TELLEZ-CASTRO; MOJICA-NAVA, 2019; ESTEVEZ et al., 2021). Hybrid approaches involving UAVs and ground vehicles (UGVs) have also been explored to take advantage of both aerial and terrestrial mobility.

When payloads are suspended from UAVs by cables, the system can be modeled similarly to a pendulum, introducing passive degrees of freedom that influence flight stability. Unwanted oscillations during flight can degrade performance and increase the risk of collisions. Control techniques have been developed to minimize these oscillations

and stabilize the system (BRANDÃO et al., 2022). In extreme cases where the UAV lacks sufficient thrust to lift a payload vertically, alternative strategies such as lateral dragging across a surface have been proposed as a viable transport method.

Research on UAV-based transportation has also extended to specialized applications, including urban package delivery, where drones navigate dense environments to deliver goods efficiently (KOTARU; WU; SREENATH, 2018). In agricultural applications, UAVs equipped with spraying systems have demonstrated their ability to cover large areas efficiently while minimizing chemical exposure to humans (TANG; WÜEST; KUMAR, 2018). In military and emergency scenarios, UAVs have been deployed for the rapid delivery of medical supplies or equipment in conflict zones and disaster-stricken regions (GUERRERO et al., 2015).

1.1 Methods for Load Transportation

The transportation of cargo using UAVs can be performed by cable-suspended loads or loads attached directly to the UAV's body, as affirmed by Villa, Brandao e Sarcinelli-Filho (2020). Each approach presents distinct advantages and challenges, impacting the drone's stability, maneuverability, and energy efficiency.

One of the key advantages of employing a cable-suspended system for cargo transportation is the flexibility it offers in maneuvering. This method allows the UAV to carry larger or irregularly shaped loads that may not be feasible to attach directly to the drone's body. Additionally, it enables cooperative transportation, wherein multiple UAVs share the load, thereby increasing the payload capacity beyond the limitations of a single drone. However, this approach introduces significant challenges concerning stability and control. The suspended load behaves similarly to a pendulum, introducing passive degrees of freedom that may result in undesired oscillations during flight. Effectively managing these oscillations necessitates advanced control strategies to ensure precise load handling and prevent excessive swinging, which could compromise safety and operational efficiency.

Conversely, directly attaching the load to the UAV's body provides greater stability, as the cargo remains rigidly fixed, eliminating the pendular motion associated with suspended loads. This characteristic simplifies control, particularly in confined or obstacle-rich environments. Moreover, this configuration allows for more aggressive and agile maneuvers, as the UAV does not need to counteract the dynamic effects of a swinging load. Nevertheless, this approach also presents drawbacks. The added weight alters the UAV's center of gravity, increases its moments of inertia, and restricts its ability to execute rapid attitude adjustments. Additionally, this method imposes constraints on the size and shape of the cargo, requiring it to be compact and appropriately positioned to avoid interference with the drone's aerodynamic performance and propulsion system.

Both methods involve trade-offs between maneuverability, payload capacity, and energy efficiency. While cable-suspended loads enable higher payload capacities and cooperative transport, they require complex stabilization systems. In contrast, attached loads enhance control and agility but impose limitations on the drone's maneuverability, reducing its responsiveness during navigation. As discussed, the advantages and disadvantages of each approach are application-dependent and must be considered based on the operational requirements.

In this study, both techniques are examined, and the rationale for their selection is clearly articulated. The comparative advantages and limitations of each approach are analyzed in relation to the specific problem addressed and the operational context in which they are applied.

1.2 Challenges in Cargo Transportation with Drones

The use of drones in cargo transportation has been rapidly expanding, bringing innovation and efficiency to logistics. However, the nature of the transported cargo directly influences the operational and technical challenges that must be overcome. In the most common case, the transportation of solid cargo, such as packages, offers greater predictability in handling and stability during flight. However, the shape of the cargo can introduce aerodynamic challenges, increasing drag and energy consumption. Additionally, securing the cargo must be carefully managed to prevent unexpected displacements, especially when the cargo is transported via suspended cables. Furthermore, weight limitations remain a critical factor, as commonly used drones support significantly lower loads compared to traditional transportation means such as cars or trucks.

On the other hand, transporting liquid cargo presents unique challenges due to the internal movement of the liquid, a phenomenon known as the slosh effect, which can significantly compromise flight stability. This issue requires the use of compartmentalized tanks or active stabilization systems, which are often associated with advanced control strategies. Additionally, variations in the center of gravity caused by liquid displacement can affect drone dynamics and stability, making UAVs an excellent testbed platform for control strategies.

In the case of variable-weight cargo, such as partially consumed liquid tanks or equipment that releases or collects materials during the flight, new operational challenges arise. Weight changes during flight directly affect energy consumption and drone autonomy, necessitating a dynamic control system that allows real-time adjustments. The stability of the equipment can also be compromised if the redistribution of weight is not well managed, making it necessary to employ systems that automatically adjust weight distribution to prevent critical imbalances.

Thus, we understand that cargo transported by UAVs can vary in nature and complexity. Solid payloads, such as packages for delivery services, are commonly used in logistics applications (KOTARU; WU; SREENATH, 2018). Liquid payloads, including pesticides and fertilizers, are particularly relevant for precision agriculture, where UAV-based spraying enhances efficiency and minimizes human exposure to harmful substances (TANG; WÜEST; KUMAR, 2018). Moreover, payloads with variable weight, such as pesticide tanks that deplete during flight, introduce additional challenges in flight stability and control. Monitoring payload weight in real-time is crucial for optimizing UAV performance and ensuring uniform application, as conventional methods based solely on nozzle flow rates may lead to inefficiencies (MOGILI; DEEPAK, 2018).

In tasks involving load transportation, a UAV carrying a cargo must adapt to changes in its dynamic model, as the added mass alters flight characteristics (VILLA; BRANDAO; SARCINELLI-FILHO, 2020). Increased thrust requirements lead to higher energy consumption, reducing flight time and operational efficiency. Consequently, cooperative transportation strategies, involving multiple UAVs or UAVs working in tandem with ground vehicles, have been explored to distribute the load and enhance transport efficiency (CARDONA; TELLEZ-CASTRO; MOJICA-NAVA, 2019; ESTEVEZ et al., 2021). Furthermore, research has demonstrated that stabilizing cable-suspended cargo can be treated as a pendulum-stabilization problem, where control techniques mitigate undesired oscillations (BRANDÃO et al., 2022).

In this context, this dissertation presents several contributions to the field of UAV-based transportation and spraying. First, a sensor capable of dynamically measuring payload weight during flight was developed, enabling real-time adjustments to spraying parameters. Second, a UAV spraying system integrated with the developed load sensor was implemented to optimize liquid distribution. Third, a vision-based approach was introduced to enhance spraying efficiency by detecting and targeting specific areas requiring treatment. Finally, cooperative UAV–ground vehicle strategies for suspended cargo transportation were investigated, demonstrating the feasibility of multi-robot collaboration in complex logistical scenarios. The findings derived from these studies provide insights for future research on autonomous decision-making, adaptive control, and the integration of heterogeneous robotic systems for large-scale agricultural and logistics applications.

1.3 Research Objective, Question, and Hypotheses

In the context presented thus far, this dissertation aims to enhance the efficiency, precision, and sustainability of UAV-based aerial spraying and cargo transportation by integrating sensing technologies, computer vision techniques, and cooperative multi-agent strategies. The research focuses on developing and validating novel methods to optimize UAV operations, improve resource utilization, and minimize environmental impact.

In summary, this dissertation seeks to answer the following research question:

How can UAV-based technologies improve efficiency, precision, and sustainability in aerial spraying and/or cargo transportation through sensing data, computer vision, and cooperative multi-agent strategies?

To address this research question, the following hypotheses are formulated:

- **H1:** A dynamic payload weight sensor integrated into UAV systems will significantly improve the accuracy of in-flight weight measurements, enabling real-time adjustments that enhance operational efficiency and resource optimization.
- **H2:** A UAV spraying system that continuously monitors and adjusts spray parameters based on real-time payload weight measurements will achieve more uniform application and reduce chemical waste compared to traditional flow-rate-based approaches.
- **H3:** The incorporation of computer vision for target detection in UAV spraying systems will enable selective pesticide application, reducing chemical usage and minimizing environmental impact while maintaining or improving crop treatment effectiveness.
- **H4:** A cooperative UAV-UGV strategy for suspended cargo transportation will enhance operational efficiency by leveraging UAV agility for aerial transport while utilizing UGVs for stability and load management in complex environments.

The alignment between the research question and hypotheses will guide the development of this dissertation, aiming to provide insights into potential advancements in UAV-based logistics and precision agriculture.

1.4 Organization of the Dissertation

This dissertation contributes to UAV-based transportation and aerial spraying by addressing key technological advancements. First, a sensor was developed to measure payload weight dynamically during flight, enabling real-time adjustments to spraying parameters. Conventional methods estimate pesticide application rates based on nozzle flow rates, which may result in inefficiencies if actual payload weight variations are not considered. The proposed sensor enhances precision in chemical dispersion, optimizing resource utilization and minimizing environmental impact.

Building upon this contribution, a UAV spraying system was developed and integrated with the load sensor to enhance liquid distribution. By continuously monitoring

the remaining payload weight and dynamically adjusting the spray rate, the system achieves greater application uniformity, ensuring consistent treatment across agricultural fields. Furthermore, a vision-based approach was incorporated to refine spraying efficiency through computer vision techniques that identify and target specific areas requiring treatment. This selective application strategy reduces chemical waste, mitigates environmental contamination, and contributes to increased agricultural productivity.

Beyond aerial spraying, this dissertation also investigates cooperative UAV-ground vehicle (UGV) strategies for suspended cargo transportation. While UAVs offer agility, their payload capacity and flight endurance impose limitations. By integrating UAVs with UGVs, operational efficiency is improved, particularly in environments where aerial transport is advantageous but requires ground-based support. This work proposes and evaluates control strategies that enable UAV–UGV collaboration for stable and coordinated payload transport in dynamic scenarios.

To systematically address these topics, this dissertation is structured as follows. Chapter 2 presents the UAV spraying system, emphasizing the impact of real-time payload monitoring on application efficiency and providing experimental validation. Chapter 3 extends this system by incorporating computer vision for target identification, enabling optimized pesticide application. Finally, Chapter 4 explores UAV–UGV cooperative transportation strategies, focusing on control mechanisms for stabilizing suspended cargo and ensuring efficient delivery under dynamic conditions.

2 Enhancing UAV Spraying Efficiency through Payload Sensor Integration

This chapter is based on the study published in the 2024 Latin American Robotics Symposium (LARS) (BARCELOS et al., 2024a), which focuses on improving UAV-based spraying operations by integrating a payload weight sensor that enables real-time adjustments to spraying parameters. Conventional pesticide application methods often rely on predefined nozzle flow rates, which do not account for variations in payload weight during the mission. By implementing a real-time monitoring system, the UAV dynamically stops the spraying task, based on the remaining liquid volume, ensuring optimized resource utilization, reduced chemical waste, and enhanced environmental sustainability.

The main objective of this work is to increase the efficiency and precision of agricultural spraying tasks by leveraging sensor data to enhance UAV navigation and control. The study specifically addresses the challenges associated with transporting a liquid payload, whose mass continuously decreases during the spraying process. This variation in payload weight directly affects the UAV's center of gravity, flight dynamics, and energy consumption. To mitigate these effects, an adaptive control strategy is proposed to dynamically adjust UAV flight parameters in response to real-time payload variations. Experimental validation demonstrates that this approach improves operational autonomy, enhances distribution accuracy, and prevents inefficient pesticide dispersion.

From a cargo transportation perspective, this research is closely related to the transport of variable-mass liquid loads, which are attached directly to the UAV's body. Unlike suspended cargo, an attached liquid payload impacts the UAV's balance and maneuverability as its weight decreases over time. These continuous changes in mass distribution influence the vehicle's stability. So, the proposed system ensures that as the liquid payload is depleted, the UAV dynamically adjusts its flight behavior, optimizing energy efficiency while maintaining accurate pesticide application.

In summary, this chapter builds upon the foundations of UAV-based precision agriculture, demonstrating how real-time payload monitoring can significantly enhance the efficiency and reliability of UAV spraying operations.

2.1 The Case-Study

Figure 3 illustrates the proposed experimental setup, in which a UAV autonomously performs an aerial spraying task. Throughout the mission, the system continuously monitors the pesticide level in the tank. When it detects that the pesticide is nearly depleted,

the pump is automatically turned off to prevent damage and reduce waste. At the start of the operation, the UAV takes off from the base with a full tank and moves to the first crop row, initiating the spraying process as long as the liquid weight remains above the predefined minimum threshold. Upon reaching the end of each row, the pump is deactivated, and the UAV repositions itself at the beginning of the next row. When the payload sensor detects that the tank is empty, the UAV records its current position and returns to the base. After refilling, it resumes the mission from the saved location. This process repeats until all crop rows are fully sprayed. The detailed sequence of actions is summarized in the eight main steps listed below.

1. **System Initialization**
    - UAV is prepared with a full pesticide tank.
    - System checks if pesticide level is sufficient.
2. **Mission Start**
    - UAV takes off from the base.
    - Navigates to the beginning of the nearest crop row.
3. **Spraying Under Crops**
    - If pesticide weight is above the minimum threshold:
        - Turn on the pump.
        - UAV flies slowly and smoothly under the crop row.
        - Gradual decrease of tank weight is monitored.
4. **End of Row**
    - UAV reaches the end of the current row.
    - Pump is turned off to avoid spraying outside crop area.
5. **Next Row Navigation**
    - UAV moves to the beginning of the next crop row.
    - If pesticide is still available:
        - Pump is turned on again.
        - Spraying continues.
6. **Low Pesticide Detection**
    - If payload sensor detects tank empty:
        - UAV saves current position.

  - Returns to base for refill or ends mission.

7. **Refill or End Decision**
   - At base:
     - If refilled, UAV resumes from last saved position.
     - Else, mission ends.
8. **Mission Completion**
   - Task is completed when UAV finishes spraying the last crop row.

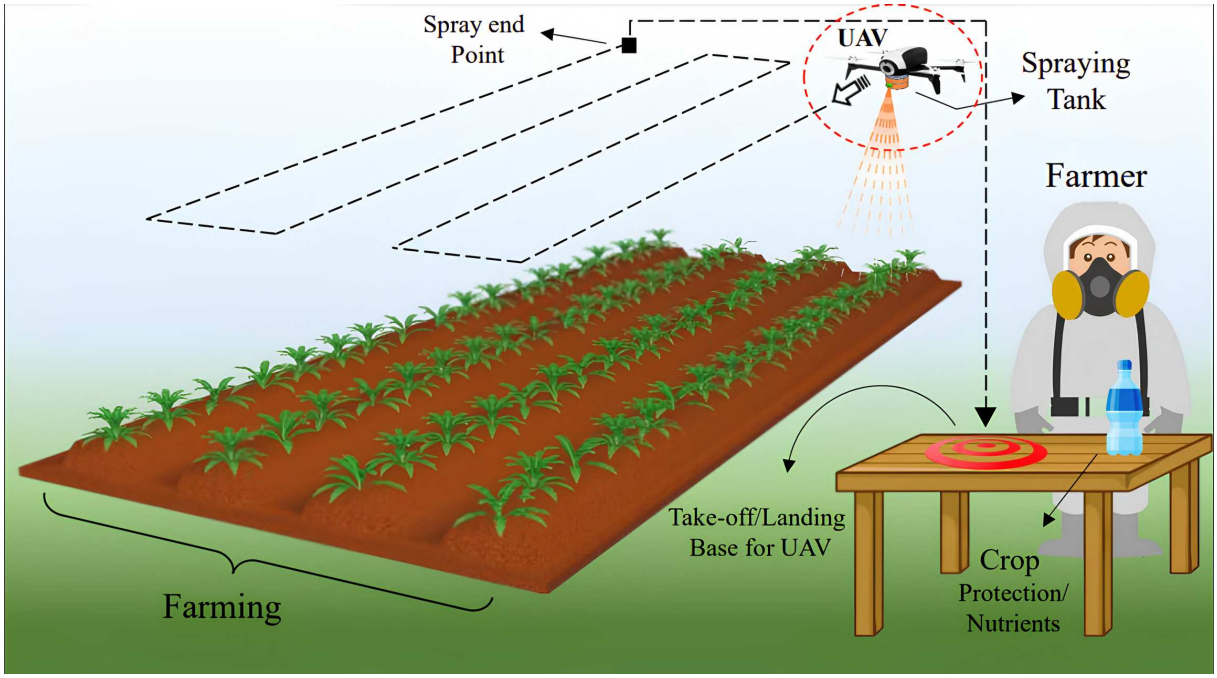

Figure 3 – Theoretical demonstration of the spraying system in a crop field.

2.2 The Spraying System

This study aimed to develop an automated aerial spraying system capable of precisely applying pesticides or nutrients beneath plant leaves. The prototype was designed to receive remote control signals, allowing activation and deactivation of the pump at optimal moments during UAV operation. The system was equipped with a 1 kg load cell to measure the liquid weight in the reservoir, enabling real-time monitoring of the payload mass during flight. Experimental validation employed a Mini Submersible DC Water Pump powered at 3.3 V, with an estimated liquid flow rate ranging from 80 to 120 L/h. Figure 4 illustrates the developed setup, where all electronics were relocated to the top of the UAV to balance the counterweight generated by the tank.

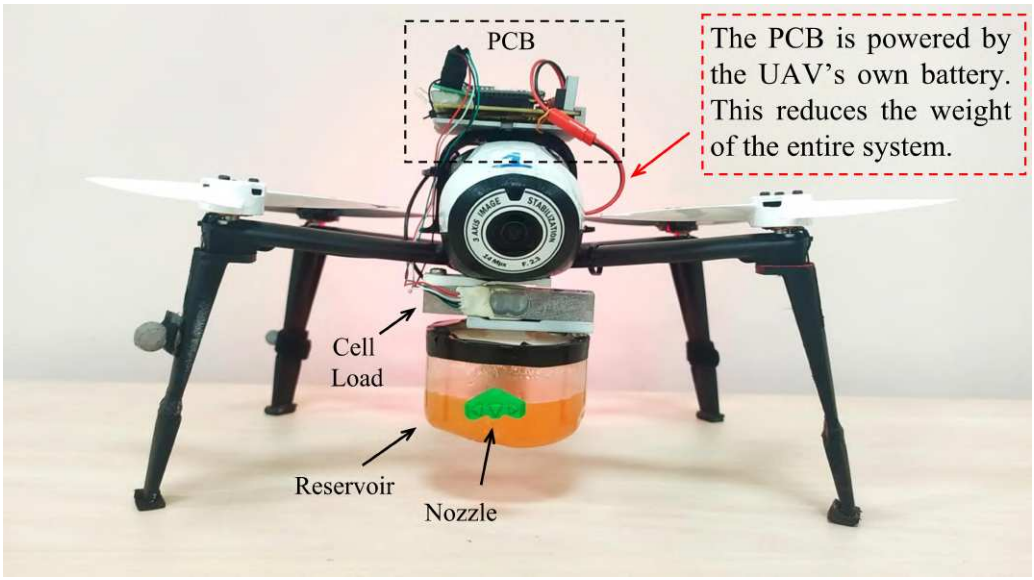

Figure 4 – Spray system reservoir and command and control system mounted on the UAV's structural chassis, showing the compact design that integrates perfectly with the drone's structure.

The UAV's posture was tracked using the OptiTrack© motion capture system, composed of 15 cameras distributed throughout the experimental arena. The motion capture data were used to estimate the position and attitude of all elements in the experiment, updating the control signals of both the UAV and the printed circuit board (PCB). Communication between the on-board system and the control station was managed through the Robot Operating System (ROS), running on a computer with Ubuntu 18.04 LTS (Bionic Beaver) and ROS 1. High-level control algorithms were implemented in MATLAB©, and integration between MATLAB© and ROS was achieved through a proprietary library that emulates ROS nodes and threads.

The system manages critical information such as the DC pump's state, the load cell readings, and the status of the digital ports controlling an RGB LED. The LED provides a visual indication of the pesticide level: a steady green light indicates a level above 30 grams, a flashing red light indicates between 30 and 15 grams, and a steady red light denotes a level below 15 grams.

To coordinate the UAV during the spraying task, communication between the on-board sensors and the Parrot Bebop 2 UAV was established via the AuRoRA (Autonomous Robots for Research and Application) framework (PIZETTA; BRANDAO; SARCINELLI-FILHO, 2016). AuRoRA allows real and simulated experiments with UAVs and UGVs using a unified MATLAB environment, facilitating the implementation of advanced control strategies.

The control system was built around an ESP32-DevKit V1 microcontroller, enabling real-time monitoring of the tank weight and the logical state of the pump. The hardware configuration includes a 1 kg load cell, an LM 7805 voltage regulator to stabilize

the power supply, and a 24-bit HX711 converter module interfacing with the load cell. A C1815 NPN BJT transistor controls the switched output signals, while a mini 3.3 V DC pump functions as the actuator, and an RGB LED provides visual feedback on system operation. These components can be seen in Figure 4.

The PCB draws power directly from the UAV's battery, eliminating the need for an auxiliary source and thereby improving payload efficiency. Further details regarding the tank development and its operational strategy are provided in (BARCELOS et al., 2024b).

The spraying mechanism consists of 3D-printed structural parts and electronic boards responsible for load measurement and signal transmission to the control station, as shown in Figure 5. The mechanical design ensured proper balance of the added payload on the Parrot Bebop 2 UAV. The tank was positioned to be visible from the onboard camera, allowing visual confirmation of the pesticide flow during operation. The PCB was mounted above the UAV frame, while the reservoir was attached to the lower structure to maintain stability.

It is worthy mentioning that the load measurement system was calibrated using a commercial precision scale as a reference, with 1 g sensitivity and a maximum capacity of 10 kg. The calibration involved correlating the load cell output with reference readings for weights ranging from 0 to 1 kg, both ascending and descending. This procedure enhanced the accuracy and reliability of the measurements, ensuring that the load cell output accurately represented the actual liquid weight in the tank.

2.3 The UAV Navigation Control

It is crucial to recognize that validating the onboard system for autonomous UAV spraying relies on the weight of the pesticide and the specific coordinates of the target location. While this article does not extensively cover the stability design and verification of the controller, these aspects are thoroughly discussed in (SANTANA; BRANDÃO; SARCINELLI-FILHO, 2016). Nevertheless, for the sake of clarity and ease of implementation, this subsection briefly outlines the UAV model and its navigation guidance controller.

The position of the UAV is described using the coordinates $\mathbf{x} = \begin{bmatrix} x & y & z \end{bmatrix}^\top$ for its translation, and the vector $\boldsymbol{\eta} = \begin{bmatrix} \phi & \theta & \psi \end{bmatrix}^\top$ for its rotation. These rotations are based on the Tait-Bryan angles of rotation, tilt, and yaw, respectively, relative to the global frame.

The built-in firmware of the Bebop 2 drone enables its autopilot to maintain flight stability by simplifying the formulation of equations that model the drone's behavior, particularly during challenging tasks. This simplified modeling approach makes it easier to design the flight controller. In this way, the drone's dynamic model can be succinctly

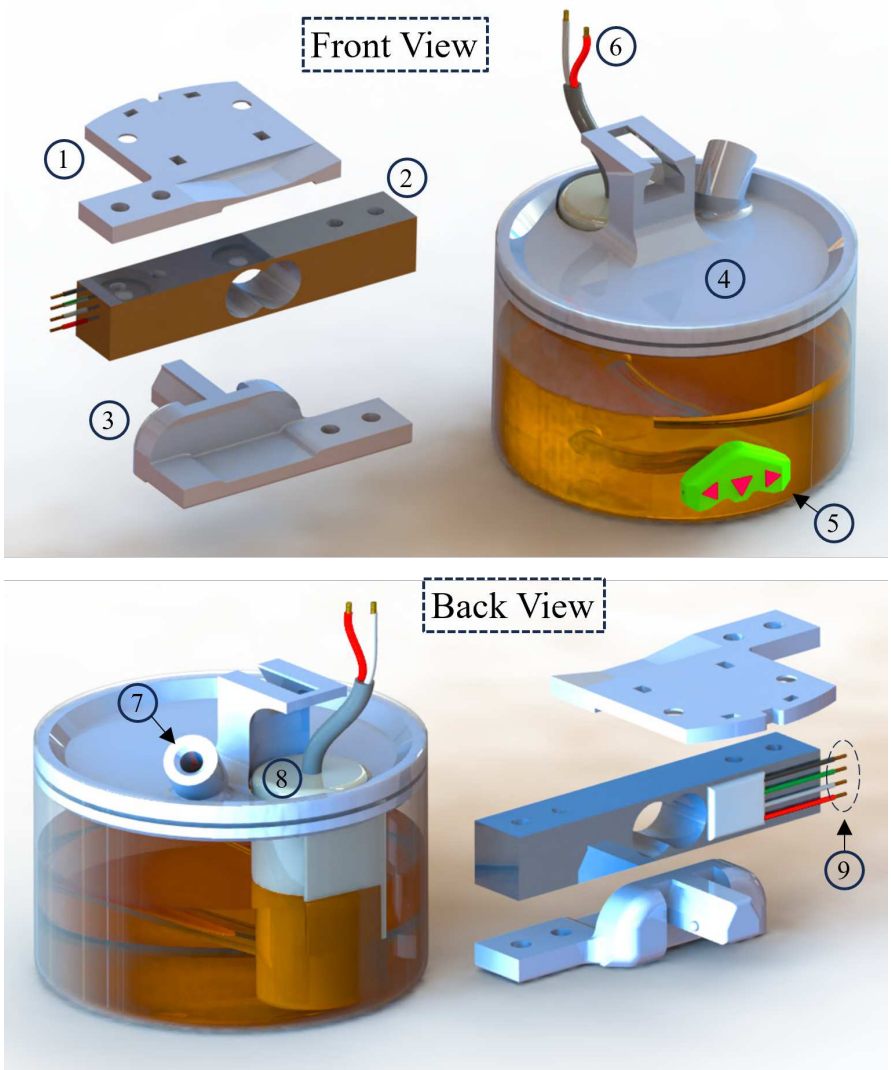

(a) Main components: 1. UAV support; 2. load cell; 3. load cell support; 4. reservoir cover; 5. nozzle with three outlets; 6. pump feed line; 7. refilling port; 8. pump; 9. load cell connection.

(b) Spraying system mounted on the UAV.

Figure 5 – Developed spraying system reservoir and integration with the UAV.

and simplified as described in (PINTO et al., 2020) and expressed as

$$\begin{bmatrix} \ddot{x} \\ \ddot{y} \\ \ddot{z} \\ \ddot{\psi} \end{bmatrix} = \begin{bmatrix} k_1 c_\psi & -k_3 s_\psi & 0 & 0 \\ k_1 s_\psi & k_3 c_\psi & 0 & 0 \\ 0 & 0 & k_5 & 0 \\ 0 & 0 & 0 & k_7 \end{bmatrix} \begin{bmatrix} u_{v_x} \\ u_{v_y} \\ u_{\dot{z}} \\ u_{\dot{\psi}} \end{bmatrix} - \begin{bmatrix} k_2 c_\psi & -k_4 s_\psi & 0 & 0 \\ k_2 s_\psi & k_4 c_\psi & 0 & 0 \\ 0 & 0 & k_6 & 0 \\ 0 & 0 & 0 & k_8 \end{bmatrix} \begin{bmatrix} v_x \\ v_y \\ \dot{z} \\ \dot{\psi} \end{bmatrix}, \tag{2.1}$$

Let's denote $c_\cdot = \cos(.)$ and $s_\cdot = \sin(.)$ for compact notation. We have $\ddot{\mathbf{q}} = \mathbf{F}_1\mathbf{u} - \mathbf{F}_2\mathbf{v}$. Here, $\mathbf{u} \in [-1, 1]$ represents the normalized control signals. Specifically, u_{v_x} and u_{v_y} correspond to pitch and roll commands, indirectly influencing the linear velocity along the x_B and y_B axes. Additionally, $u_{\dot{z}}$ and $u_{\dot{\psi}}$ are related to the inputs for $\dot{z}$ and $\dot{\psi}$ respectively. Finally, v_x, v_y, and $\dot{z}$ denote the linear velocities along the x, y, and z axes in the UAV body frame, while $\dot{\psi}$ represents the angular velocity around the z axis in the global frame.

It is important to emphasize that, based on (SANTANA; BRANDÃO; SARCINELLI-FILHO, 2016), although the model does not encompass the dynamics of the UAV, this formulation aims to illustrate the impact of high-level control signals on the vehicle's maneuvers.

To perform a path-following task, the control law

$$\mathbf{u} = \mathbf{F}_1^{-1}\left(\boldsymbol{\eta} + \mathbf{F}_2\mathbf{v}\right), \quad \text{with} \quad \boldsymbol{\eta} = \ddot{\mathbf{q}}_d + \mathbf{K}_d\dot{\tilde{\mathbf{q}}} + \mathbf{K}_p\tilde{\mathbf{q}}, \tag{2.2}$$

guides the UAV. Where $\tilde{\mathbf{q}} = \mathbf{q}_d - \mathbf{q}$ is the posture error, and $\mathbf{K}_d$ and $\mathbf{K}_p$ are positive defined gain matrices.

The algorithm presented in Algorithm 1 outlines the logic for executing the UAV-based spraying mission. The procedure begins by initializing the Bebop UAV, ROS communication, the OptiTrack tracking system, and the spraying system, which includes a load sensor and pump. The UAV is then checked for connectivity and battery level. If the system is ready, the UAV takes off and starts the spraying task. To make the task clearer, Figure 6 shows the flowchart of the actions carried out in the spraying task proposed in this document.

During the mission, as long as the time, battery voltage, and current tank mass (m_{CT}) meet predefined conditions, the UAV moves to the first garden bed while continually updating its position and control states. The UAV monitors its location relative to the garden bed; if positioned correctly, the pump activates to start spraying. The pump turns off once the UAV reaches the end of the bed, and the drone proceeds to the next one. Once the mass of the empty tank (m_{ET}) has been preset, if the tank becomes empty, ($m_{CT} < m_{ET}$), the system stops spraying and the UAV returns to the starting position.

2.4 Results and Discussions

To experimentally validate our spraying strategy, an experiment with three 3 m long beds was designed following the principles described in Figure 3. The results about the variation of carried mass are presented in Figure 7 and the link of the video demonstrating the experimental validation of our case study can be found in <https://youtu.be/0EBBKq-HEIs>. Algorithm 2 describes the logic adopted to carry out the spraying mission, observing the reading status of the mass transported by the UAV (in lines 9 and 22, m_{CT} and m_{ET} stand for current mass in tank and empty tank mass, respectively). Figure 8 shows the three-dimensional route taken by the UAV during the proposed spraying mission. It can be seen that the desired route covers the entire

Algorithm 1 Structure of System Control to Task.

```
1: Initialize the Bebop UAV and ROS Communication
2: Initialize the tracking system by OptiTrack
3: Initialize the System Spraying (load sensor and pump)
4: Enable Emergency bottom
5: Takeoff Bebop and Start the Spraying Task
6: while t < t_max & Battery level > 10% & m_CT > m_ET do
7:   if Permition of Execution then
8:     Go to the beginning of the first garden bed
9:     Get Pose data and Update the UAV states
10:    Compute the Control Signals
11:    if Exist commands from Joystick then
12:      Override autonomous controller with Joystick info
13:    end if
14:    Get Sensor Load data (mass and state pump)
15:    if UAV over garden bed then
16:      Turn on pump
17:      Update the path to UAV
18:      if UAV arrives at the end of garden bed then
19:        Turn off the pump
20:        UAV go to the next garden bed
21:      end if
22:      if m_CT < m_ET then
23:        Turn off the pump
24:        Return to home and Finish Task
25:      end if
26:    end if
27:    Sent control signals to UAV
28:    Store state variables
29:    if Permition for plotting in real-time then
30:      Display the Graphical Simulation
31:    end if
32:  end if
33: end while=0
```

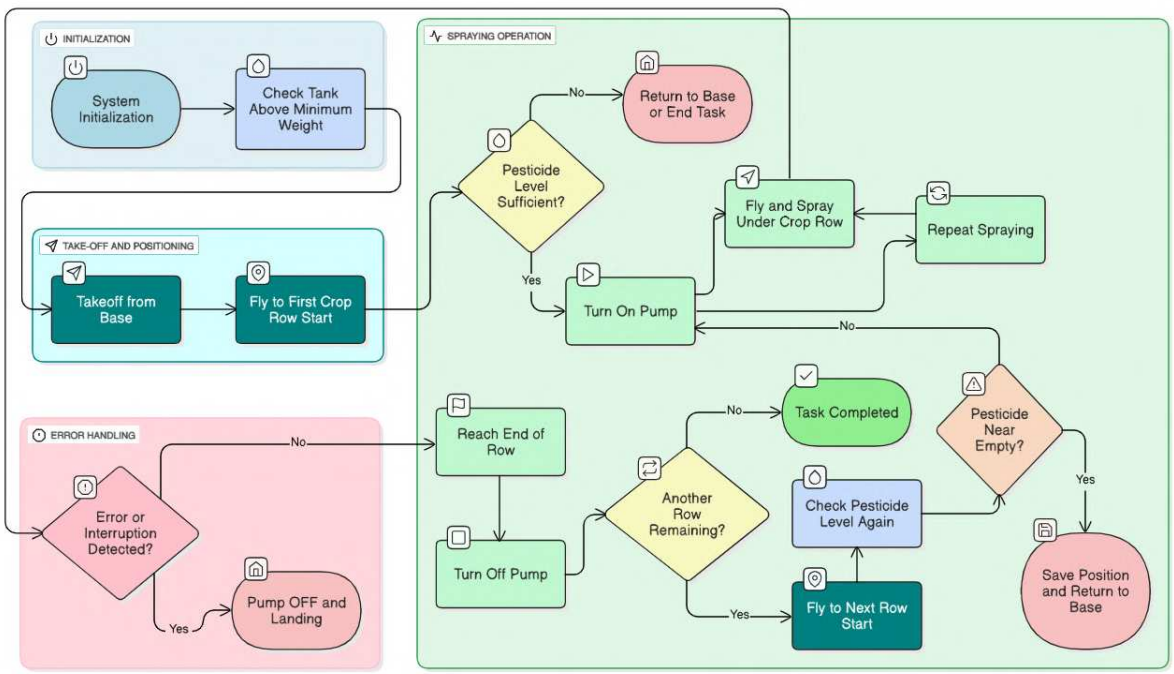

Figure 6 – Fluxogram to decribe about the steps related with the Spraying Task.

plantation (see the signal $\mathbf{x_d} = \begin{bmatrix} x_d & y_d & z_d \end{bmatrix}^\top$), but the route taken by the UAV stops earlier, as the cargo contained in the container runs out and the UAV finishes the mission by returning to base.

The system takes approximately 4 seconds to fully initialize and calibrate, which explains the absence of readings during this period (as indicated by the gray region in the graph). Additionally, for safety, we set a minimum weight of 15 grams to ensure that the pump never operates empty, regardless of the UAV's inclination during maneuvers. Furthermore, as long as the sensor indicates values above 15 grams, the UAV is permitted to take off and begin spraying. The prototype tank was filled with approximately 100 grams, as confirmed by the load signal between 4 and approximately 9 seconds, during which the UAV took off from the takeoff/landing base and heads towards the nearest plot following a predefined route with constant velocity. At 9 seconds, the UAV is vertically positioned over one end of the bed, and the pump is activated, as indicated by the green region from 9 to 23 seconds. The weight in the reservoir gradually decreases during this time interval, confirming that the liquid is being dispersed. At 23 seconds, the UAV is positioned above the opposite end of the bed, and the pump is deactivated until the UAV reaches the next bed according to the route. At this point, the first bed is completely sprayed, and the current tank capacity is at 50% of the initial quantity, indicating that approximately 50 grams of pesticide and 14 seconds were required to spray a bed completely. At 28 seconds, spraying of the second bed begins and continues until 41 seconds, at which point the weight reading reaches our empty tank value (15 grams), and the pump is turned off as the UAV returns to the base and completes its mission.

It is worth noting that the peak in weight recorded at 41 seconds is due to the UAV maneuvering, as its return speed is higher than its speed during spraying. At 44 seconds, the UAV lands at the base, and we observe that the sensor still registers approximately 10 to 15 grams in the tank. It is worth mentioning that during the path tracking presented, the UAV maintained its orientation constant, aiming to optimize the energy consumption of the battery. Thus, the spraying of the second bed was done in reverse.

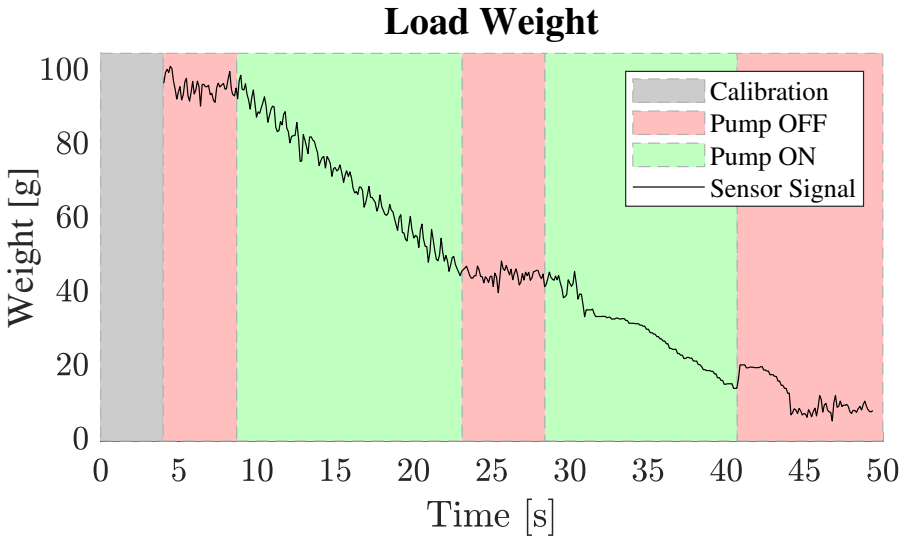

Figure 7 – Variation in the weight of the pesticide during the experiment.

At the end of the analysis, we observed that the maximum weight transported by the UAV was 278 grams, with 178 grams attributed to the spraying system and 100 grams to the liquid payload. This means the UAV successfully carried approximately 52.45% of its own weight. It is worth mentioning that the drone's internal controller compensates for altitude variation, thereby adjusting for changes in the mass of the spray tank during flight. Futhermore, the primary objective of this work was to develop a prototype for autonomous spraying that can be easily attached to the drone's body, eliminating the need to control the flow rate at the tank nozzle. This design choice explains why the duration of the experiment was limited to less than one minute.

2.5 Concluding Remarks

This study describes a UAV-based spraying system designed for pesticide distribution, with the aim of optimizing resources and potentially increasing crop health and productivity. The experimental results validate the operational functionality of the onboard water pumping mechanism and the precise measurement of the weight of the pesticide carried by the UAV.

The use of UAVs can bring additional benefits, such as reducing direct human exposure to agricultural pesticides and minimizing inadvertent contact with plants, thus

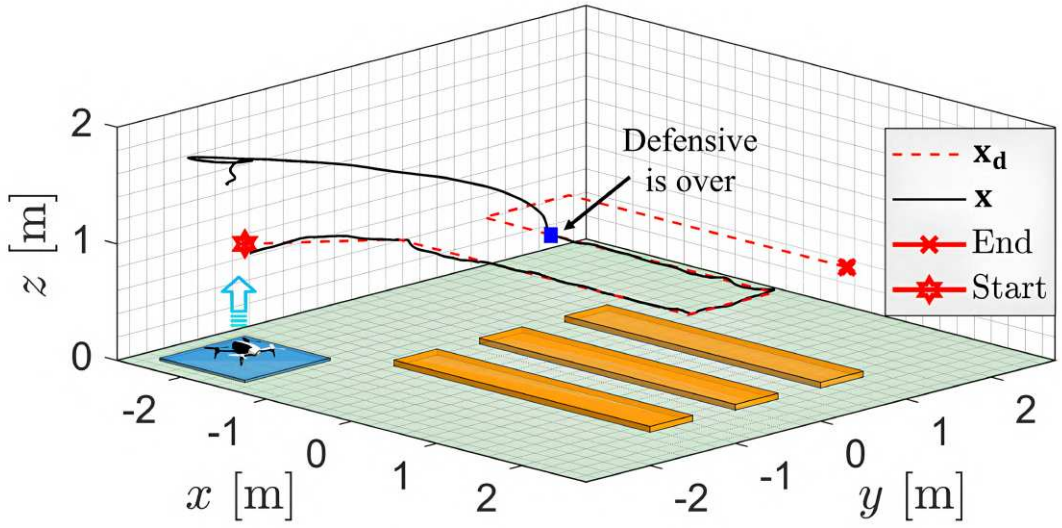

(a) Isometric View.

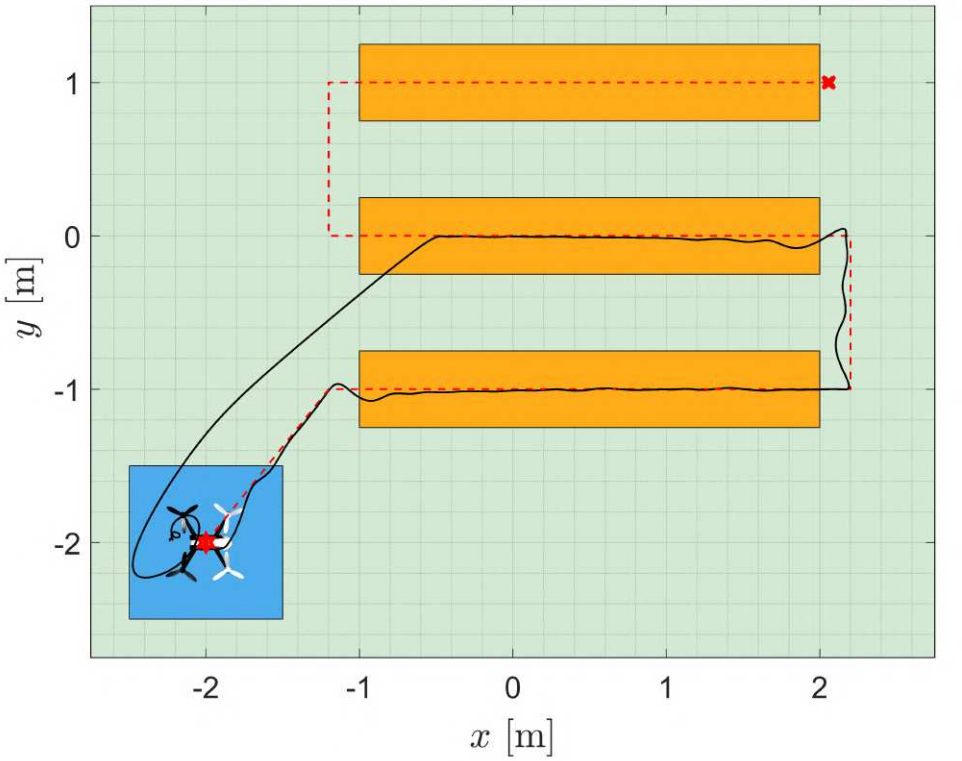

(b) Superior view.

Figure 8 – Behavior of UAV's positioning during the Spraying Task.

avoiding delays in plant development. Therefore, continuous research and the development of cost-effective technologies are imperative in order to take advantage of UAVs in Precision Agriculture.

For future advances in this field, we propose increasing the efficiency of the system by integrating an autonomous refueling mechanism. When the UAV detects a drop in pesticide levels, it will autonomously return to base for refueling. As the tank is refilled,

the weight of the system gradually increases and, when maximum capacity is reached, the UAV resumes spraying from exactly where it left off. Alternatively, an empty tank could be exchanged for a full tank upon the UAV's arrival at the refuelling station, minimizing downtime.

In addition, a servo-visual controller could be employed for the precise identification of planting beds, allowing targeted application based on real-time detection of start and stop points. By using the navigation data, we could further analyze the UAV velocity to dynamically adjust the spray rate in relation to its speed. This would ensure an optimal application of pesticides, where the spraying intensity is adjusted based on the UAV's movement, enhancing both efficiency and coverage.

3 Integration of Payload Sensors UAV-Based Spraying

This chapter is based on the study published in *Drones 2024* (BARCELOS et al., 2024b). The research presents a load measurement system to dynamically adjust defensive distribution, complemented by an image segmentation model to classify plants (healthy, sick or absent), improving spraying efficiency while reducing chemical waste and environmental impact. This approach optimizes UAV-based precision agriculture by integrating real-time payload monitoring.

A key contribution of this work is the development and validation of a prototype payload sensor integrated into a UAV spraying system. The UAV follows a predefined path-planning strategy, utilizing image processing to detect plant diseases. Once a diseased plant is identified, the UAV pauses its route and activates the spraying mechanism, ensuring targeted defensive application rather than indiscriminate spraying. The real-time payload sensor continuously monitors the defensive levels, determining whether the UAV should continue the operation or return to the base station for refueling.

The experimental validation was conducted in a controlled environment, repeating the task to evaluate variations in the payload's initial condition: empty tank (requiring return for refueling), full tank (operating without the need for refueling), demonstrating that the UAV's flight controller successfully maintained stability despite challenges posed by liquid oscillations and varying payloads. The results confirm that real-time payload monitoring enables more accurate defensive application, reducing unnecessary waste and improving UAV operational efficiency. Furthermore, from a cargo transportation perspective, the study also highlights the impact of variable-mass liquid loads attached directly to the UAV's body.

In summary, this work contributes to the advancement of UAV-based agricultural spraying by integrating sensor-driven real-time adjustments to enhance precision, efficiency, and sustainability in modern farming practices.

3.1 The Case Study

Figure 9 illustrates the practical scenario studied in this work, in which the UAV performs an autonomous inspection task of a vegetable garden, which can be extended to larger crops. Given the arrangement of plants in the beds, where they are usually equally spaced from each other occupying the entire length of the bed, the UAV must optimally cover the entire cultivated area, monitoring the health of the plants. In this sense, the

UAV follows a path composed of uniformly spaced points at a fixed height, generating straight segments connected by smooth curves. It should be emphasized that the list of points was ordered to allow continuous drone navigation under all beds, that is, once a bed has been inspected, the UAV must move to the nearest bed. Furthermore, the UAV's yaw orientation must be tangent to the curves that connect the beds in order to maintain the same displacement pattern (moving forward) while navigating and during the transitions between the beds, otherwise there would be beds where the drone would return backwards. Once it has taken off from the takeoff/landing platform, the UAV heads towards the first point of the path, and upon reaching this position, it must pass under the first bed at a constantly steady speed to ensure the sharpness of the captured photos. Upon reaching the last point of the path, the inspection is completed and the UAV returns to the base to end the task.

The UAV's spraying system is designed to operate based on the amount of defensive in the tank. The pump activates when the tank's weight is above a predefined minimum threshold, allowing the UAV to distribute the defensive over the crops. As the liquid level decreases, the system continues spraying until the tank's weight nears the empty reservoir's weight. At this critical point, the UAV records its current position and returns to the base to prevent damage to the pump and conserve battery power. The farmer then has the option to refill the tank and resume spraying from the last saved location or to end the task. The monitoring and spraying process is considered complete once the UAV finishes the final crop row.

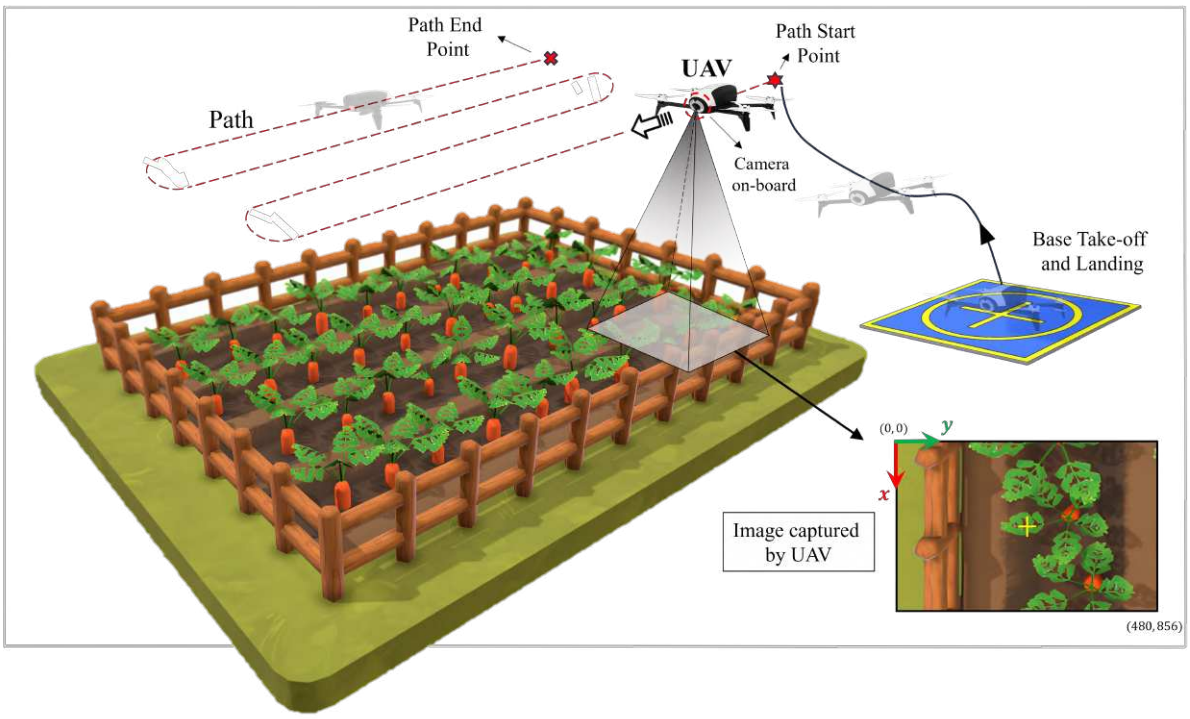

Figure 9 – Illustration of the task of real-time monitoring of a carrot crop using the proposed path-following approach.

Figure 10 illustrates the photo-capturing strategy. When flying at an altitude of 1.5 m above the plant beds, the captured images often contained more than one plant. However, the classification algorithm was designed to analyze only the plant located directly beneath the UAV and disregard any others. To achieve this, the image processing procedure was configured to frame the target plant at the center of the image, considering the known camera resolution of (480×856) pixels, 14 megapixels, and a sampling rate of 5 frames per second. After each photo was captured, a (150×150) pixel region was cropped around the image center to verify the presence of a plant. If a plant was detected, the algorithm evaluated whether it was healthy or diseased. Upon identifying a diseased plant, the UAV paused its trajectory and initiated the spraying process over the affected area.

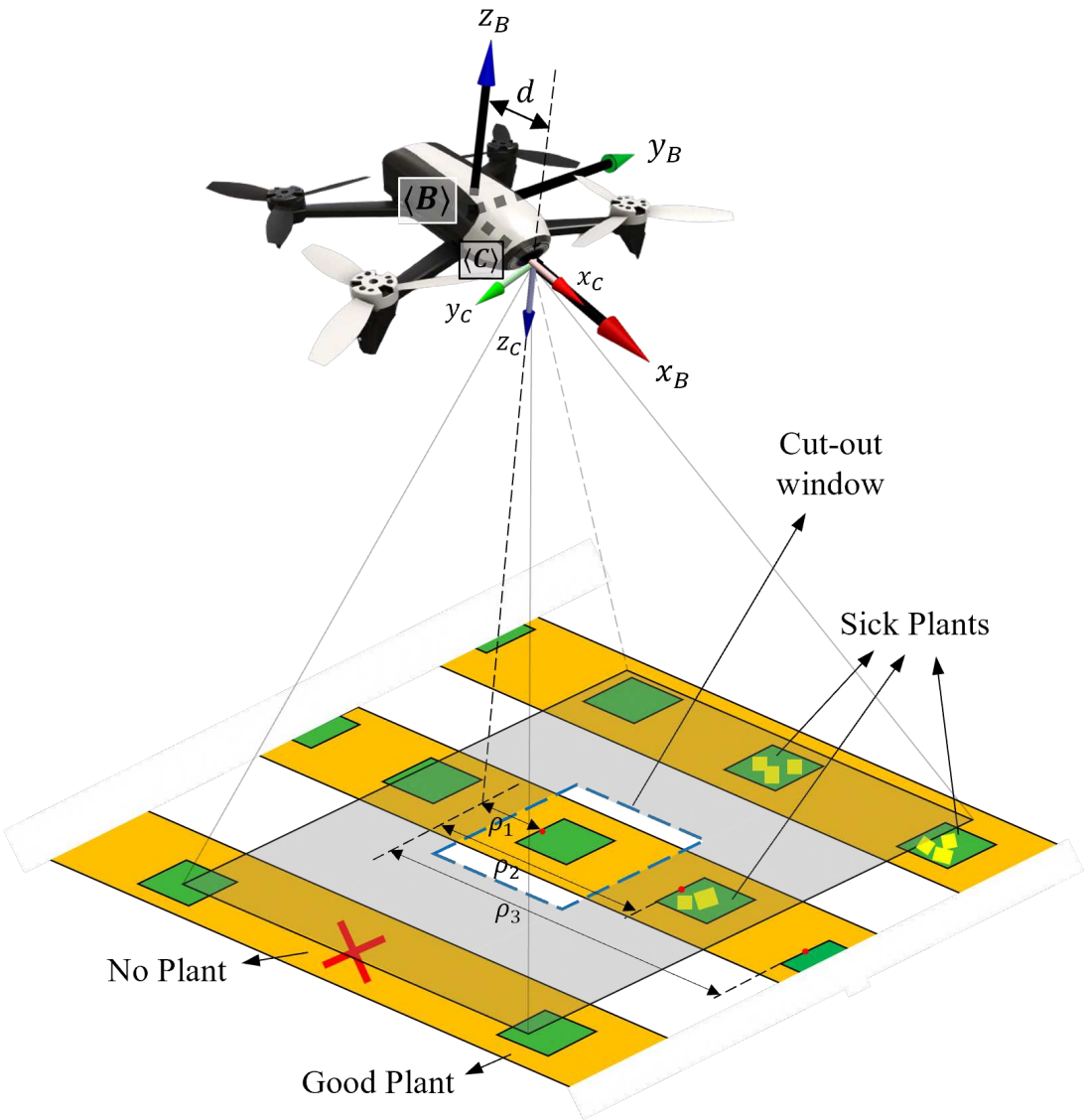

Figure 10 – Reference system for Parrot Bebop 2 UAV using Tait-Bryan angles.

3.1.1 The Monitoring Strategy

Firstly, it is important to note that the UAV's on-board camera is displaced by about 10 cm along the x_B axis of the UAV's center of mass (the origin of the UAV's reference system), as illustrated previously in Figure 10. Therefore, a homogeneous transformation between the camera reference system ($\langle \mathbf{C} \rangle$) and the UAV reference system ($\langle \mathbf{B} \rangle$) was necessary to accurately determine the corrected geometric location of the drone. Given that the position of each plant was known due to standardized planting, the condition required to capture images with the plants centered on the image plane was based on the positional error between the UAV and each plant. Specifically, let $\tilde{\boldsymbol{\rho}} = \begin{bmatrix} \rho_1 & \rho_2 & \dots & \rho_n \end{bmatrix}^\top$, where $\rho_n = \mathbf{x}_{UAV} - \mathbf{x}_{plant_n}$. The image capture process was allowed whenever $\tilde{\boldsymbol{\rho}}$ was less than $\rho_{min} = 10$ [cm]. A binary vector checks plant visitation, ensuring that each plant is photographed only once.

Our monitoring proposal basically involves identifying the presence of plants in the center of the images and assessing their condition. Image processing consists of three fundamental steps: image capture, cropping and feature extraction. First, photos are taken to ensure that the UAV is positioned above the plant, using the position error between the drone and each plant, as discussed in section 3.1. As several plants can appear in the image, the target plant for analysis is the one located in the center of the image plane, i.e. 10 cm from the UAV's current position. The algorithm cuts the image around the center to focus on the desired plant. The cropped image is then converted from the RGB color scale to HSV to facilitate the application of a segmentation mask, which identifies green tones to confirm the presence of a plant. Another mask is applied to detect yellow tones, indicating the presence of a diseased plant directly below the drone. The result of the algorithm for each image is a Boolean vector that indicates whether a plant is present in the captured image and whether it is diseased. To avoid noise in the detection process, the presence of green or yellow was only considered significant if the segmented area exceeded 20 pixels^2. Finally, diseased plants are highlighted by coloring the edges of the yellow regions in red.

3.1.2 The Control Strategy

Successful autonomous UAV spraying hinges on factors including defensive mass and target location geometry. While this paper focuses on the spraying system, the reader is referred to (SANTANA; BRANDÃO; SARCINELLI-FILHO, 2016) for in-depth controller design and stability analysis. Note that the controller used in this work is the same as that presented and discussed in the previous chapter, so here we will refrain from demonstrating its stability.

Algorithm 2 and the Figure 11 outline the logic and the specific actions for executing the spraying mission, incorporating real-time monitoring of the UAV's payload.

Algorithm 2 Structure of Control System.

```
Initialize ROS Communication, tracking system (OptiTrack) and Bebop UAV
Initialize the Spraying device (load sensor and pump)
Takeoff Bebop and Start the Monitoring Mission
while !(Route Accomplished) & !(Empty tank) do
    Monitor the plantation (Image processing)
    if Sick Plant detected then
        Pause path tracking
        Execute spraying
        if Defensive Amount reached then
            Stop spraying
            Resume path
        end if
    else
        Follow the path
    end if
    Get Sensor Payload data
    if Tank is empty then
        Return the base to refill tank | Finish the mission
    end if
    Get Pose data and Update the UAV states
    Compute the Control Signals
    if Exist commands from Joystick then
        Override autonomous controller with Joystick info
    end if
    Sent control signals to UAV
    Store state variables
end while=0
```

3.2 Results and Discussion

In this section, a proof-of-concept experiment was conducted using two simulated garden beds, each with 3 meters in length. Plant models were created using EVA leaves of varying sizes (0.4 , 0.30 , and 0.20) and colors (light and dark green) to represent different crop types. Plants were spaced 0.5 apart, totaling 11 plants (with one intentional gap, no plant). The experimental validation video can be accessed via the following link: https://youtu.be/lB_JT8X3N-8.

The image processing algorithm was responsible for classifying the plants as healthy, sick or absent. Figure 12 shows examples of these categories, with the corresponding segmentation results displayed in the bottom row. Note that the irrigation nozzle is visible in the photographs captured by the UAV; however, it was intentionally moved back to avoid overlapping the mechanism on the plants in the cropped image in the center of the photographs (as indicated by the blue square). The images in the second row show the result of our segmentation, where we highlighted the presence of green, yellow or black colors, which allowed us to identify and classify the health of the plants analyzed.

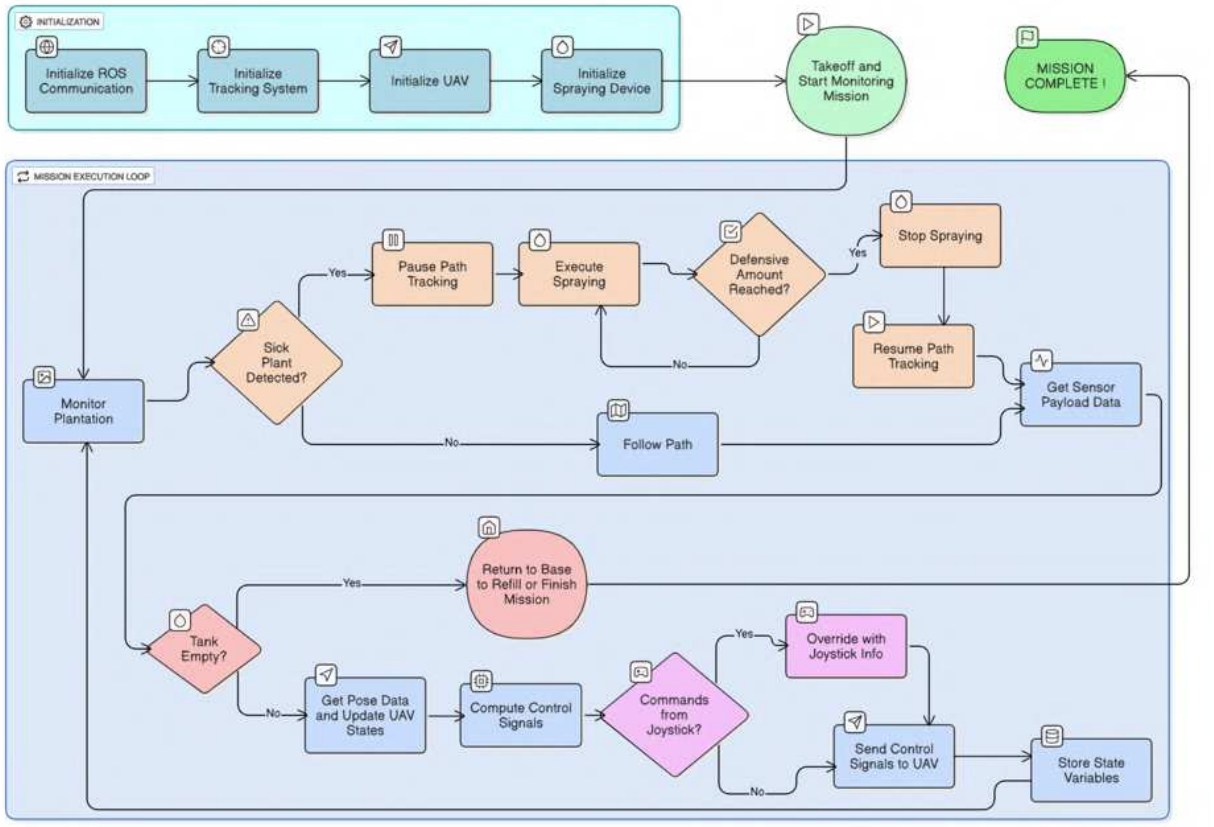

Figure 11 – Flowchart describing the main actions involved in the spraying task, using the UAV's onboard camera to detect diseased plants.

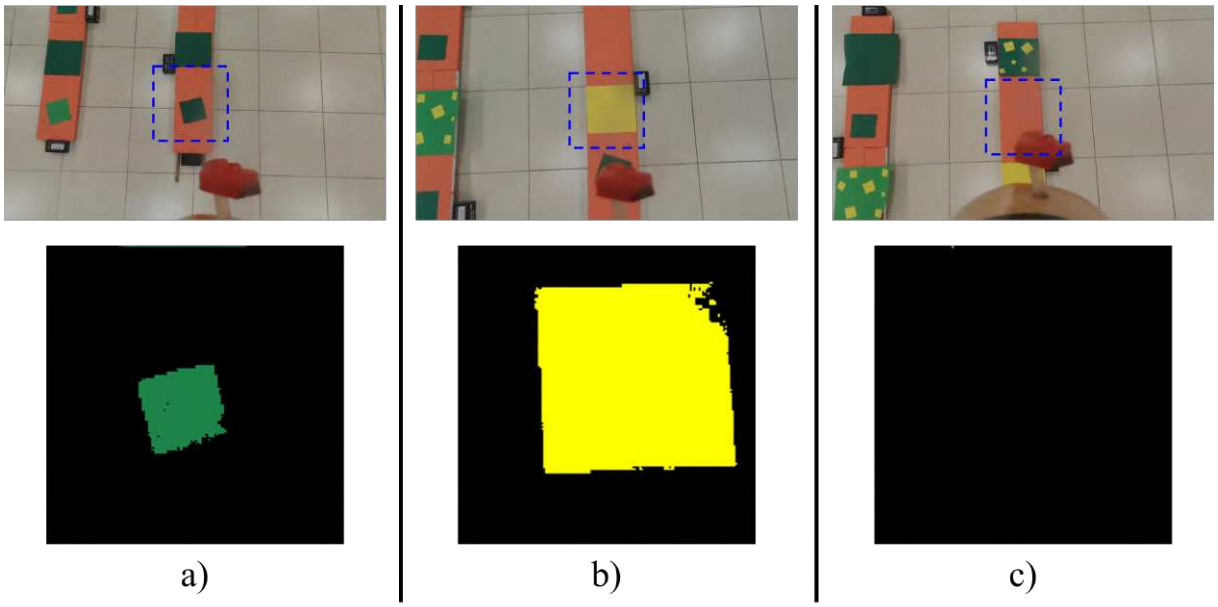

Figure 12 – Captured Photos and Segmented Images. a) Good Plant. b) Sick Plant. c) No Plant.

Figure 13 illustrates the variation in payload, as well as the times when the pump was activated and deactivated during the real-time experimental validation of the proof of concept. The periods labeled Calibration, Pump OFF and Pump ON are highlighted in

grey, green and red, respectively. These labels correspond to the time required to calibrate the load cell after initialization and the periods when the pump was switched on and off. During the Calibration stage, it is not possible to determine the weight available in the tank, which explains the absence of a signal during this process. Both graphs show sharper variations when the UAV takes off; however, despite the initial noise, the signal stabilizes once the UAV is in flight. When the pump is activated, there is a gradual decrease in the signal over time, explained by the fact that the liquid is pumped out of the tank, thus reducing its weight. In both experiments, the same amount of defensive, 5 grams, was released on each sick plant. It is interesting to note that the time interval needed to spray the same amount of defensive varied between the experiments. The time taken to release the 5 grams on each diseased plant was longer in the first experiment compared to the second, indicating a lower flow rate out of the nozzle in the first experiment. Finally, it is worth noting that the noise observed in the signal in both graphs is caused by the vibration of the quadcopter itself in flight.

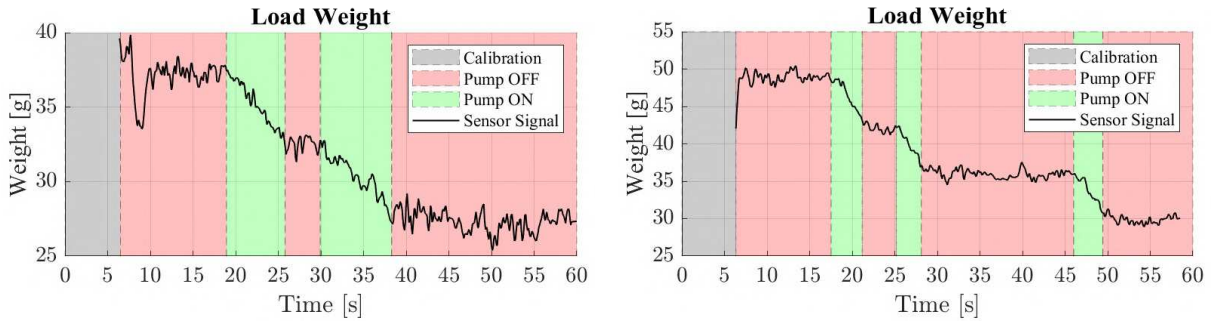

(a) Experiment 1: With refueling stop.

(b) Experiment 2: Covering the all plant beds.

Figure 13 – Evolution of Defensive Mass in UAV Tank and Corresponding Pump States.

Pump activation was contingent upon the image segmentation stage, specifically, the detection of diseased plants (yellow-colored). In the initial experiment (Figure 13a), despite identifying three sick plants, the pump operated only twice. This discrepancy arose from the load cell system indicating insufficient liquid for continued application after detecting the third sick plant, necessitating the UAV's return to base for refueling. To prevent pump damage from dry running, a weight threshold of 30 grams was established. This accounted for potential liquid displacement due to the UAV's movement. Spraying commenced only if a diseased plant was detected and the liquid weight exceeded the threshold. Otherwise, the UAV returned for refueling. In the second experiment (Figure 13b), the initial defensive load was approximately 50 grams, sufficient to cover all beds and treat the three sick plants without intermediate refueling.

The UAV's trajectory during both experiments is shown in Figure 14. In the first experiment (Figure 14a), the UAV detected insufficient defensive upon encountering the third diseased plant and returned to base for refueling. This resulted in a deviation from the planned path and omission of inspection for the remaining plants in the second

bed. Blank entries indicate that the UAV failed to pass within 0.1 m of these plants, preventing image capture and subsequent analysis. In contrast, in the second experiment (Figure 14b), the UAV successfully identified, sprayed, and classified all plants in the garden. Notably, in both experiments, the desired $\mathbf{x}_d$ and current $\mathbf{x}$ UAV positions closely aligned, demonstrating the control system's effectiveness in maintaining precise positioning, even while carrying a payload.

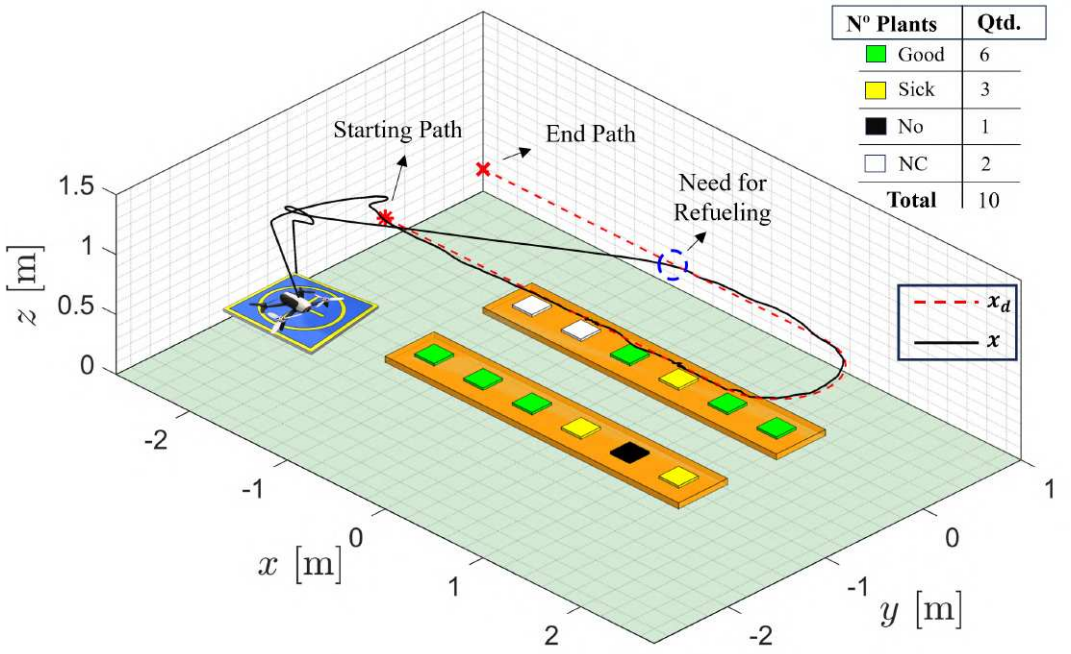

(a) Experiment 1: UAV displacement with a refueling stop..

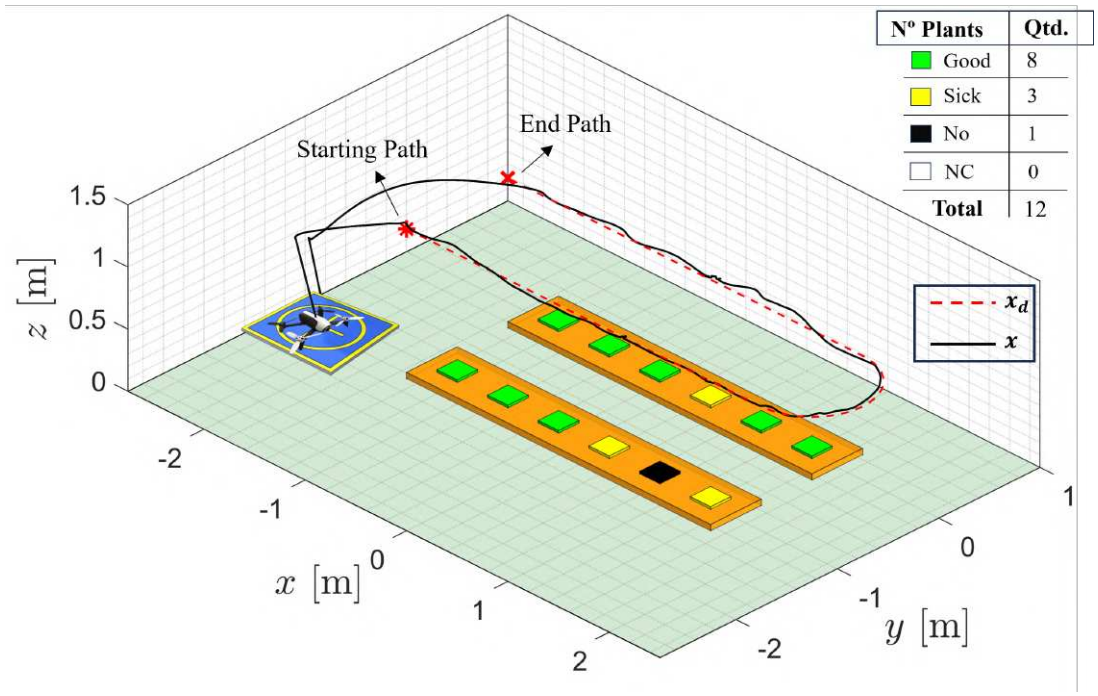

(b) Isometric view.

Figure 14 – UAV flight path with corresponding plant disease classification. Note: NO and NC means No plants and Not Computed, respectively.

The analysis revealed the UAV could carry a maximum payload of 228 grams, comprising a 178-gram spraying system and 50 grams of liquid. This load represented approximately 45.60% of the UAV's estimated 500-gram weight. This study focused on developing a self-contained spraying prototype for drone integration, prioritizing weight-based liquid dispensing over nozzle flow rate control. An RGB LED visual indicator was implemented to signal liquid levels during testing. The LED cycled through green (steady or flashing) and red to denote liquid weight above 40 grams, between 30 and 40 grams, or below 30 grams, respectively.

It is worthy to highlight that our approach can be adapted for non-liquid payloads since the load sensor functions independently of the cargo type. This versatility allows for the utilization of drones in various applications, such as seed distribution in reforestation efforts or the deployment of larvicides in water reservoirs to combat dengue and other similar diseases. This potential for diverse applications highlights the broader implications of our work in advancing UAV technology for environmental and public health initiatives.

In this work, the agricultural spraying system has been designed for targeted applications, allowing for individualized treatment of each plant. This approach stands out compared to traditional systems, primarily due to its ability to ensure that a precise and uniform amount of defensive is applied to each plant based on the weight of the applied product, rather than relying on time intervals or flow control. Unlike conventional systems that depend on the nozzle's spray rate, our system measures the actual amount of defensive deposited, guaranteeing that each plant receives the same quantity of product regardless of terrain variations, environmental conditions, or liquid viscosity. This precision is crucial in crops where uniform treatment directly affects productivity and plant health.

The measurement of the liquid's weight guarantees uniform application, avoiding both underdosing - which could compromise the treatment's effectiveness - and overdosing - which could lead to waste and undesirable environmental impacts. This optimization not only reduces the use of excess inputs, making operations more economical, but also maintains the effectiveness of the treatment.

Additionally, the proposed spraying system offers flexibility in adjusting the amount of pesticide applied to each plant according to its disease severity, as determined by the ratio of yellow to green areas in the captured images. This capability is particularly beneficial for crops requiring individualized treatment—such as orchards, vineyards, or garden cultivations—ensuring that more severely affected plants receive proportionally greater quantities of pesticide. In essence, through the use of Digital Image Processing (DIP) techniques, the system can automatically regulate the amount of pesticide released (in grams), adapting to the specific needs of each plant as well as to varying environmental conditions. However, this aspect lies beyond the scope of the present work and is suggested as a promising direction for future development.

In conclusion, additional tests were conducted to validate alternative configurations, as illustrated in the accompanying video (<https://youtu.be/IdVl9vTMFpg>). During these experiments, several variations were explored, including modifications to the control strategy, the simulated liquid dispersion system, and both the monitoring and spraying procedures. The results reinforce the effectiveness of the proposed methods and provide valuable insights into the potential of UAV-based spraying systems for precision agriculture applications.

3.3 Concluding Remarks

This study presents the development of a UAV-based spraying system designed for targeted defensive application on color-identified diseased plants, aiming to optimize resource use and improve crop health and productivity. Experimental results confirmed the effectiveness of the digital image processing technique, the functionality of the onboard water pumping mechanism, and the accuracy of the UAV's defensive weight measurement. A main contribution of this work is the integration of a real-time payload monitoring system, which continuously tracks the weight during flight to ensure precise defensive application and prevent over- or under-spraying. Additionally, the system supports automatic refueling by detecting low defensive levels and directing the UAV to return to base when needed.

In conclusion, this work demonstrates an alternative application of UAVs in agriculture. Notably, the employed technique minimizes direct human exposure to agricultural defensives and unintentional contact with crops, preventing potential developmental delays. The proposed inspection technique could be further expanded to identify mature and green plants, for example. Overall, our study contributes to the development of cost-effective technologies that maximize the potential of UAVs in precision agriculture.

Additionally, our approach can be extended to non-liquid payloads, as the load sensor operates independently of the type of cargo being transported. This enables the use of drones for seed distribution in reforestation missions or for deploying larvicides in water reservoirs to combat dengue and similar diseases.

Future research directions include conducting open-air field tests with real plants. This would introduce additional complexity due to external factors like wind gusts and varying lighting conditions. Additionally, employing RGB-D cameras would provide color and depth information, facilitating real-plant growth assessment based on height measurements using the relative distance between the drone and the top of the plants.

4 Lifting Electromagnets in Collaborative Load Transport and Delivery Tasks

This chapter is based on the study published in *Applied Sciences 2023* (BARCELOS et al., 2023), which presents a cooperative transportation strategy involving heterogeneous robotic systems, where UAVs and UGVs collaborate to overcome transportation challenges. The study addresses scenarios in which a UGV is unable to complete a delivery due to an obstacle in its path, requiring a UAV to lift and transfer the load between UGVs.

A key contribution of this work is the practical implementation of a suspended load transportation system, where a UAV equipped with an electromagnetic lifting actuator manipulates cubic packed cargo. The UAV lifts the payload from the first UGV using a cable-suspended mechanism, transports it across an impassable obstacle, and releases it onto a second UGV positioned at the destination. This method ensures that aerial transport is utilized only during critical mission phases, optimizing energy consumption while maintaining the efficiency of ground-based transport.

The experimental validation was conducted in a controlled environment, demonstrating the feasibility of UAV-UGV collaboration for cargo transportation. The results highlight the challenges associated with stabilizing a suspended load, where oscillations and pendular motion must be mitigated to ensure flight stability and accurate delivery. Additionally, the integration of electromagnetic actuation enables secure grasping and precise release of the payload, ensuring reliability in dynamic conditions.

In summary, this chapter presents the principles of cooperative transportation, showing how heterogeneous multi-robot teams can optimize load delivery operations in constrained environments. The integration of suspended load transport, structured cargo handling, and aerial-ground collaboration represents a step forward in developing scalable logistics solutions for urban delivery, disaster response, and industrial applications.

4.1 Possible Practical Applications

Some hypothetical scenarios illustrate the importance of load transportation between aerial and ground vehicles. Rescue operations, for instance, often involve situations that require the application of cargo transport techniques. In the first example, shown in Figure 15, consider an ambulance responding to a traffic accident on a heavily congested avenue or a bridge that is difficult to access. In such a case, a UAV can support emergency services by transporting first-aid supplies or specific medical devices from the nearest hospital to the accident site, facilitating faster response and potentially saving lives.

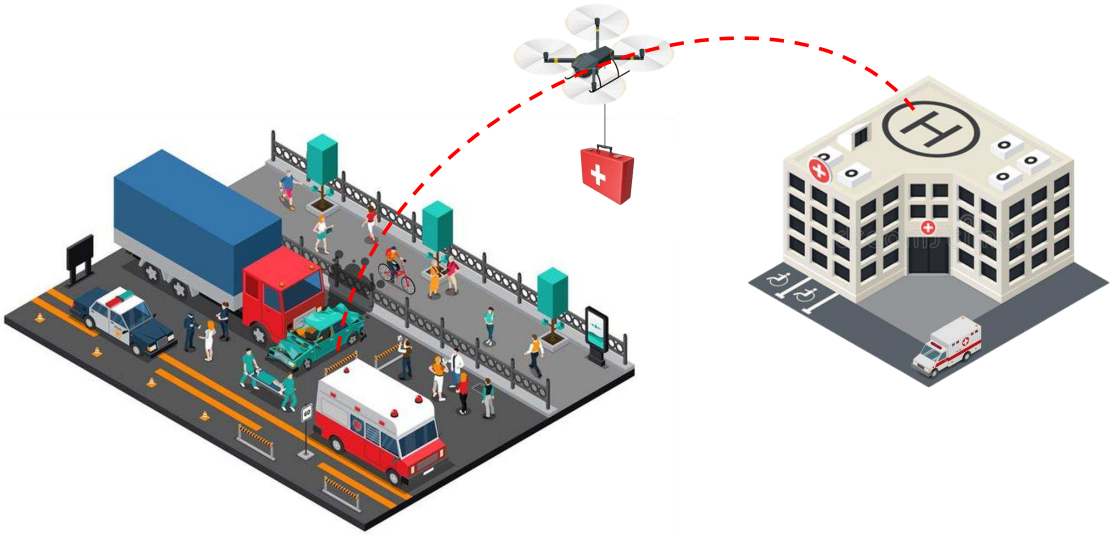

Figure 15 – Example of situation of emergency delivery.

To further complement some rescue operations, Figure 16 presents a didactic illustration of a situation in which a rescue team is trying to contain a fire in a burning building. In this hypothetical situation, there are civilians present inside the structure, and there is no easy access to the interior of the building due to the fire and the imminent risk of the structure collapsing. Once the rescue team is unable to access the interior of the building, immediate relief equipment can be sent to victims, such as a gas mask or water for example, aiming to increase the chances of rescuing a more significant number of victims still alive.

Drone deliveries are one of the main trends for the future of e-commerce. In fact, with the expansive growth of the industry in recent years, companies in the sector are looking for increasingly advanced solutions to stand out in this extremely competitive market. Given this, the delivery of products by using drones is a very promising strategy for the future (LEMARDELÉ et al., 2021).

As another practical example in a real-world scenario, imagine that a ground delivery vehicle is in transit to deliver a large number of goods. Suppose now that this vehicle is crossing a long-span bridge, at the site of a mechanical problem, congestion due to an accident, or even civic maintenance on the bridge structure. In this situation, this vehicle will be stopped on the bridge until traffic is cleared, which may seem normal as this happens with high frequency in today's urban environments. However, if we suppose that vehicle is transporting hospital supplies, such as vaccines or even human organs, we have a situation in which every second of delay could risk lives. Thinking of such situations, it is proposed that a UAV goes to the ground vehicle that is stopped in traffic. Then, it flies carrying the cargo to a desired coordinate, where there will be a third vehicle waiting for it. Figure 17 illustrates such a situation.

After presenting some hypothetical applications related to suspended load transportation with a heterogeneous robot team, we then present our cargo transportation strategy in cases where a UGV cannot fulfill a delivery task and a UAV comes to assist it in accomplishing the mission.

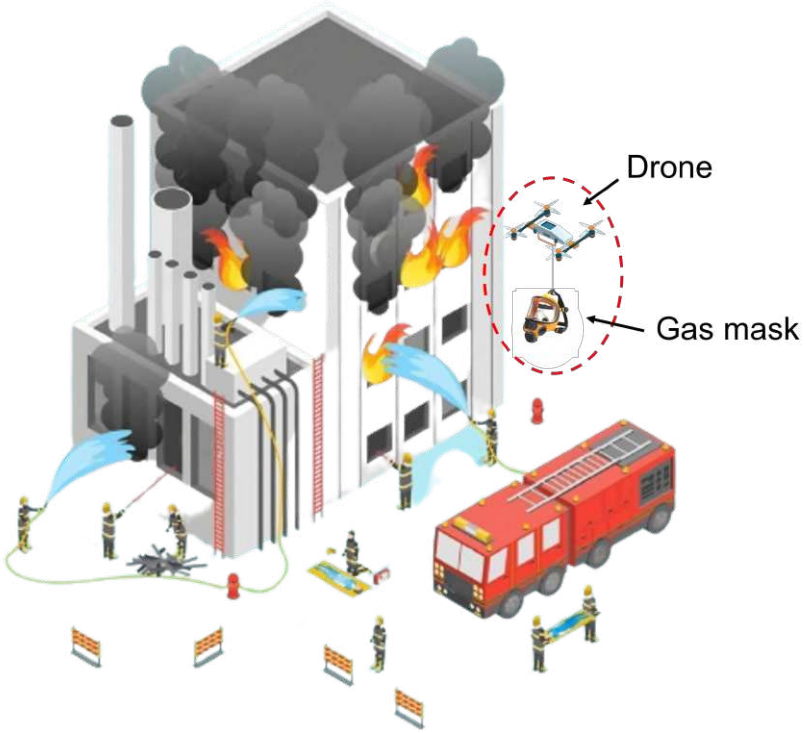

Figure 16 – Example of situation of rescue operation.

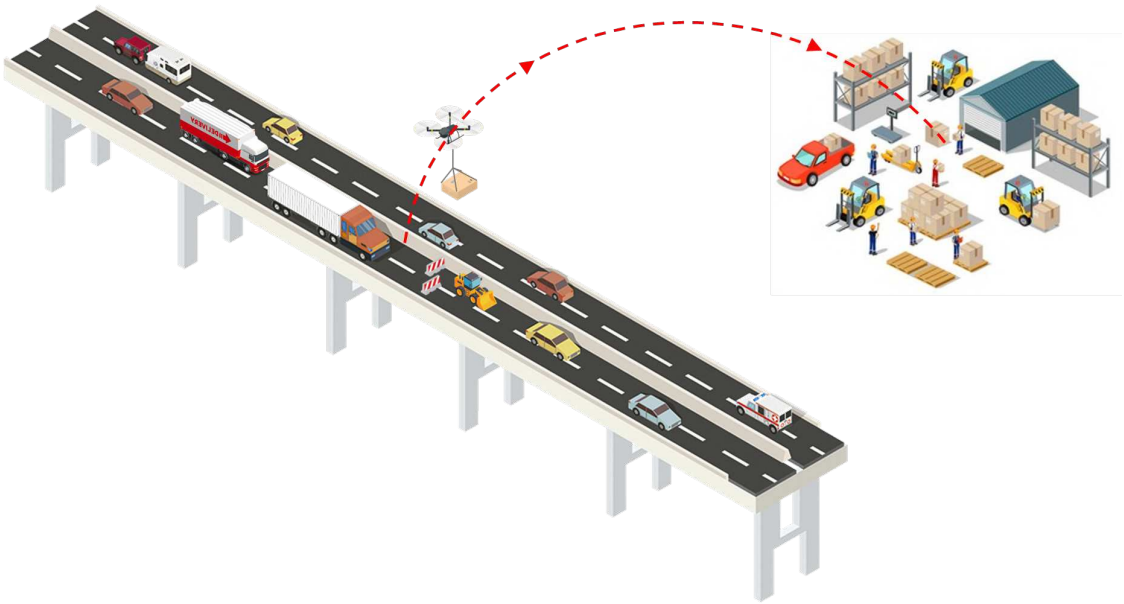

Figure 17 – Example of delivery operation when the traffic is congested.

4.2 The Cooperative Cargo Transportation Strategy

Among some applications listed, this manuscript focuses its efforts on implementing a control strategy for transport with a heterogeneous formation during lifting, transposing, and delivering loads. To stress the multirobot collaboration, we assume the environment has a physical barrier that makes it impossible for ground robots to cross from one side to another, for instance, a UGV trying to reach the opposite side of a broken bridge. Figure 18a illustrates the ground robots P1 and P2, the aerial vehicle B1, the cargo C1, and also a trailer T1 used to transport B1.

Due to the obstacle positioned between the UGVs, it is assumed that three robots are required for the practical validation of a real cargo transportation strategy: two UGVs (P1 and P2) and one UAV (B1). Since robot P1 cannot overcome the imposed barrier, robot P2 moves to the opposite side of the obstacle, reaching a predefined coordinate where it receives the load. The transfer is performed by the UAV, which lifts, transports, and delivers the cargo between the two ground vehicles.

Our delivery strategy is composed by four steps, as follows:

1: Cargo (C1) needs to be taken from city A to city B, but we previously know of the existence of a recently collapsed bridge between the two cities. A single vehicle (P1) cannot reach city B, and requires a second vehicle (P2) on the opposite side to accomplish the delivery task.

2: Once P1 arrives at the bridge, P2 is called to pick up the load on the other side of the bridge.

3: After P2 arrives to serve P1, the load must be transferred between them by using B1. With P1 and P2 waiting at rest, B1 begins the aerial transposition above the fallen bridge by picking up the load from P1 and placing it over P2. Once this is done, B1 goes back to meet P1 and lands on it.

4: After overcoming the obstacle, the cargo over P2 goes to the desired destination, whereas P1 and B1 returns to city A to receive a new delivery order.

Figure 18 presents in detail the events of the delivery task described above, and how it will be implemented in practice. Initially, Figure 18a shows the agents that compose the entire formation and how they are arranged in space. And also, see Figure 19 for a better explanation of the actions performed during the Delivery Task proposed.

Figure 18b, P1 goes to the desired target close to the obstacle. At the same time, B1 is carried on the trailer T1; note also that C1 is carried on P1. Figure 18c shows P2 starting this movement; it goes to the opposite side of the obstacle to receive C1. Then, B1 takes off to position itself over P1. After that, B1 captures C1 by using the electromagnet E1

(see Figure 18d). Now, B1 transports C1 from P1 to P2, as depicted in Figure 18e. Being over P2, B1 decouples C1 and returns to land on T1 after stabilizing the pendulum motion

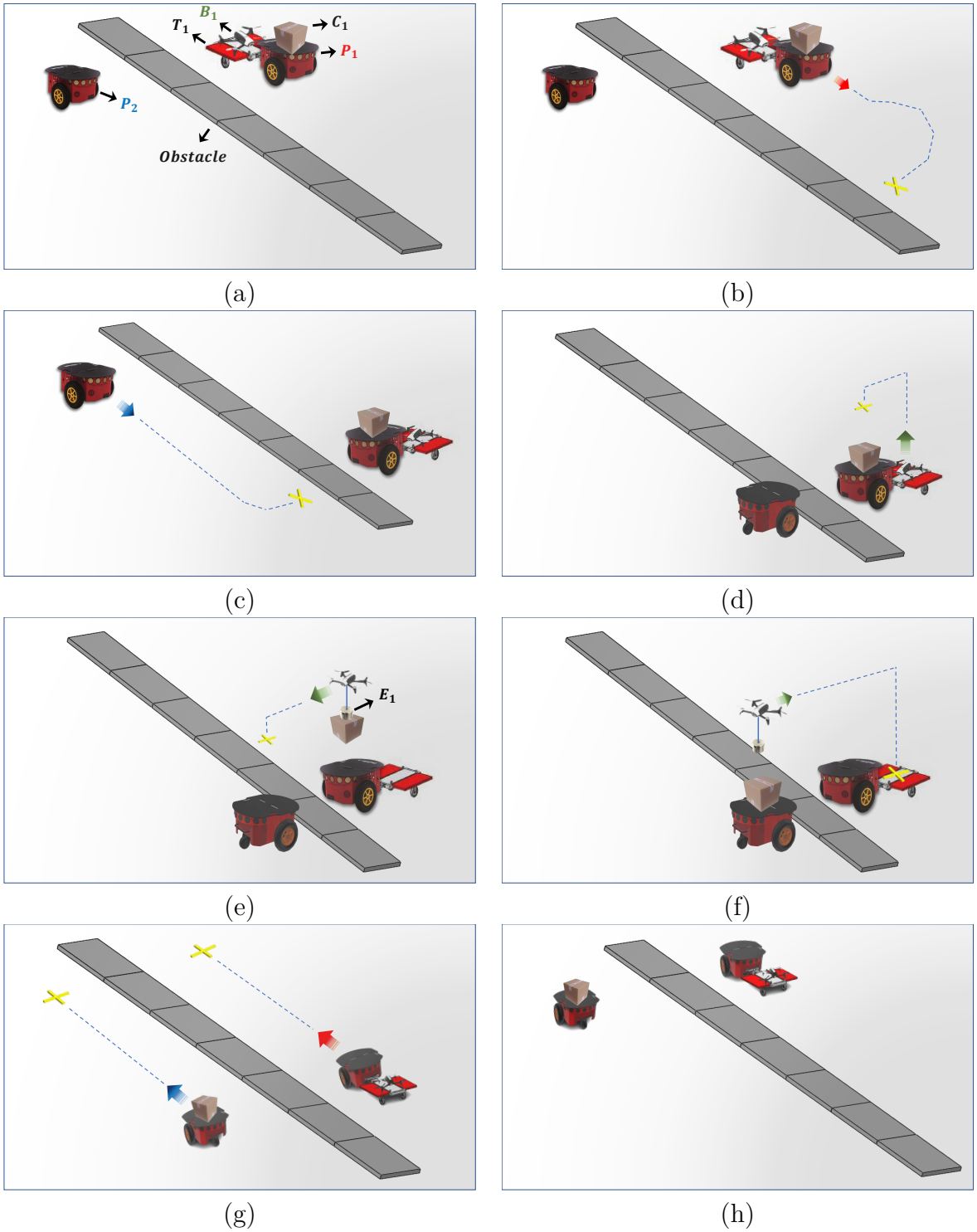

Figure 18 – Sequence of events of formation during the experiment. (a) Agents of heterogeneous formation. (b) B1 starts moving towards the desired point. (c) P2 starts its movement to give assistance to P1. (d) B1 takes off to pick up C1. (e) B1 passes with C1 under the obstacle. (f) B1 delivers C1 on P2 and returns to T1 to land. (g) All formation returns to their respective destination. (h) Task is completed successfully.

of E1 (see Figure 18f). In the sequel, P1 and P2 go to their respective pickup/delivery points (Figure 18g). Finally, the transportation task is successfully completed as shown in Figure 18h.

It is important to emphasize that P1 cannot move freely during the positioning task due to the trailer T1 attached to it. In other words, certain maneuvers, such as sharp turns, are impossible because T1 could collide with P1. To overcome this constraint, a set of waypoints was defined to produce a smooth and continuous approach maneuver, as illustrated in Figure 20. To position P1 perpendicular to the obstacle, its trajectory begins with a straight segment extending to the midpoint of the path, followed by a curved section modeled through a series of small, straight-line segments. In contrast, the path of P2 is simpler, as it only requires reaching a predefined point beside P1 and then moving toward a point near the obstacle to perform a 90° rotation and face P1. Finally, after completing the load transposition, both P1 and P2 return to their respective home positions.

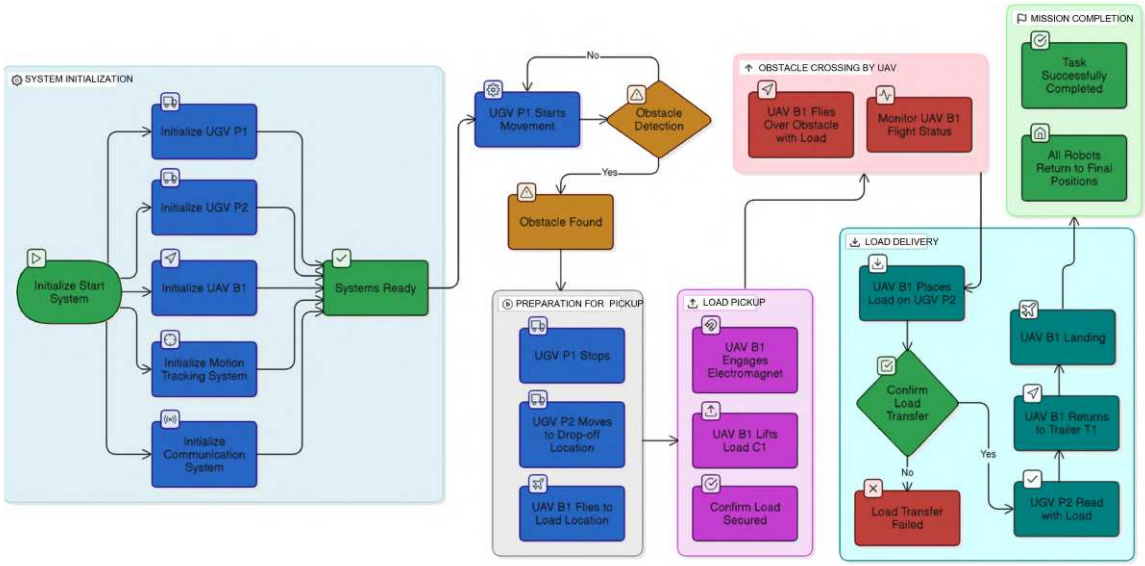

Figure 19 – Flowchart describing the actions in the UAV–UGV delivery task.

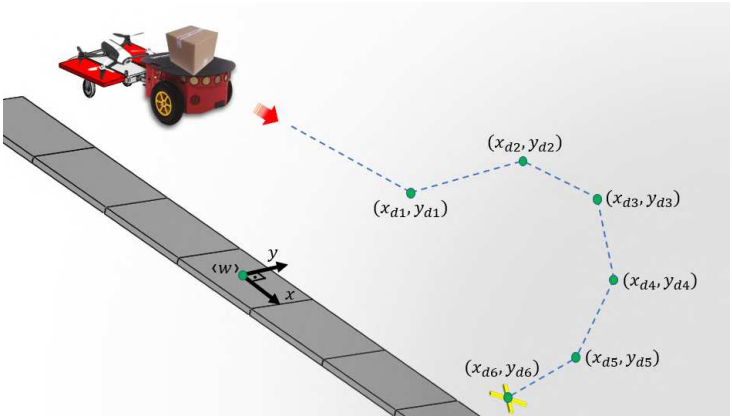

Figure 20 – Sequence of way-points implemented to performing the validation experiment and avoid collision between the B1 and T1.

4.3 Robots Modeling and Control

It is worth emphasizing that the focus of this work is the implementation of the controllers to guide a formation of ground and aerial robots cooperating in a load transportation task. Despite its relevance, the design and stability proofing of the controllers are beyond the scope of this paper. We leave for interested readers the details presented in our previous works (BRANDÃO; SARCINELLI-FILHO; CARELLI, 2013; SANTANA; BRANDÃO; SARCINELLI-FILHO, 2016). Nevertheless, to facilitate the understanding of this manuscript and, consequently, its implementation, this section brings the model of the vehicles and the controllers used to guide them.

4.3.1 The Control Strategy for the UGVs

Our UGVs are a unicycle-type mobile robot, whose kinematic model is given by

$$\begin{bmatrix} \dot{x} \\ \dot{y} \\ \dot{\psi} \end{bmatrix} = \begin{bmatrix} \cos\psi & -a\sin\psi \\ \sin\psi & a\cos\psi \\ 0 & 1 \end{bmatrix} \begin{bmatrix} u \\ \omega \end{bmatrix}. \tag{4.1}$$

Observing Figure 21, $\mathbf{x} = \begin{bmatrix} x & y \end{bmatrix}^\top$ is the robot position, ψ is its heading with respect to x-axis of the global frame $\langle W \rangle$, and a is the linear distance between the point of control and the robot axle. Finally, u and ω are its linear and angular velocities, respectively.

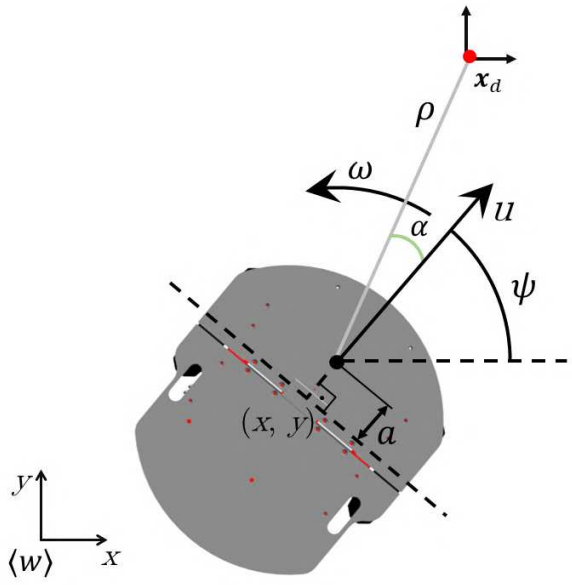

Figure 21 – The UGV seeking for its destination $\mathbf{x}_d$.

Representing the robot navigation in polar coordinates, we have

$$\rho = \sqrt{(x_d - x)^2 + (y_d - y)^2} \tag{4.2a}$$

$$\theta = \arctan \frac{y_d - y}{x_d - x} \tag{4.2b}$$

$$\alpha = \theta - \psi, \tag{4.2c}$$

where ρ is the robot-destination distance, θ is the desired orientation, and α is the heading error to the destination.

In this work, the navigation circuit is given by a set of way-points, without time constraints. Consequently, the robot performs a regulation (positioning) task, in which temporal derivatives of the reference positions are equal to zero. Having this in mind, let us take the first time derivative of (4.2). By replacing (4.1), we get the kinematic model in polar coordinates

$$\begin{bmatrix} \dot{\rho} \\ \dot{\alpha} \end{bmatrix} = \begin{bmatrix} -\cos\alpha & -a\sin\alpha \\ \dfrac{\sin\alpha}{\rho} & -a\dfrac{\cos\alpha}{\rho} - 1 \end{bmatrix} \begin{bmatrix} u \\ \omega \end{bmatrix}, \quad \text{or in the compact form} \quad \dot{\mathbf{h}} = \mathbf{B}\mathbf{u}, \tag{4.3}$$

with $\dot{\theta} = \dot{\alpha} + \omega$.

Assuming that the sequence of way-points favors task-oriented arrival, let us design a controller with no final orientation. In this case, theta is a free variable, with the constraint of being finally bounded. Thus, based on Lyapunov theory, let us take the following radially unlimited candidate function

$$V(\mathbf{h}) = \frac{1}{2}\mathbf{h}^\intercal\mathbf{h} > 0. \tag{4.4}$$

By applying the feedback linearization technique, we can propose the control signal

$$\mathbf{u} = -\mathbf{B}^{-1}\mathbf{G}\tanh\mathbf{h}, \tag{4.5}$$

with $\mathbf{G}$ being a positive defined gain matrix.

After applying its first time derivative in (4.4), and replacing (4.3) and (4.5), we get

$$\dot{V}(\mathbf{h}) = \mathbf{h}^\intercal\dot{\mathbf{h}} = \mathbf{h}^\intercal\mathbf{B}\mathbf{u} = -\mathbf{h}^\intercal\mathbf{G}\tanh\mathbf{h} < 0. \tag{4.6}$$

Therefore, it is demonstrated that the global asymptotic convergence of $\mathbf{h} \to 0$, for $t \to \infty$, which means that the robot will reach its goal in the absence of obstacles. In addition, as a consequence, $\mathbf{u} \to 0$, also for $t \to \infty$.

4.3.2 The Control Strategy for the UAV

Our UAV is the quadrotor Bebop 2, Parrot Inc., in X-configuration, whose body and global frame are illustrated in Figure 22. Its translational coordinates are defined as $\mathbf{x} = \begin{bmatrix} x & y & z \end{bmatrix}^\top$ and its attitude is described by the vector $\boldsymbol{\eta} = \begin{bmatrix} \phi & \theta & \psi \end{bmatrix}^\top$, which contains the Tait–Bryan angles of rotation, pitch and yaw, both related to the global frame $\langle w \rangle$.

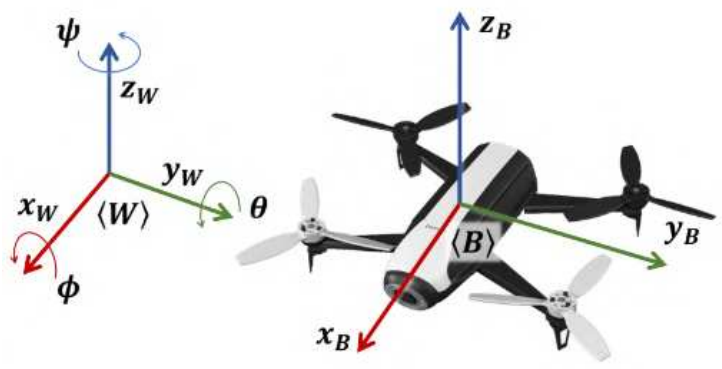

Figure 22 – Reference system for Parrot Bebop 2 UAV, according to Tait–Bryan angles.

Because Bebop 2 has an autopilot, we can assume that its in-flight stabilization is the responsibility of the embedded firmware. Consequently, for tasks performed in near-hovering operations, the UAV response can be modeled by a more simplistic set of equations, useful for the proposal of flight controllers. Given this fact, its simplified dynamic model in the global frame can be written as

$$\begin{bmatrix} \ddot{x} \\ \ddot{y} \\ \ddot{z} \\ \ddot{\psi} \end{bmatrix} = \begin{bmatrix} k_1 \cos\psi & -k_3 \sin\psi & 0 & 0 \\ k_1 \sin\psi & k_3 \cos\psi & 0 & 0 \\ 0 & 0 & k_5 & 0 \\ 0 & 0 & 0 & k_7 \end{bmatrix} \begin{bmatrix} u_{v_x} \\ u_{v_y} \\ u_{\dot{z}} \\ u_{\dot{\psi}} \end{bmatrix} - \begin{bmatrix} k_2 \cos\psi & -k_4 \sin\psi & 0 & 0 \\ k_2 \sin\psi & k_4 \cos\psi & 0 & 0 \\ 0 & 0 & k_6 & 0 \\ 0 & 0 & 0 & k_8 \end{bmatrix} \begin{bmatrix} v_x \\ v_y \\ \dot{z} \\ \dot{\psi} \end{bmatrix}, \quad (4.7)$$

or in the compact formulation as $\ddot{\mathbf{q}} = \mathbf{F}_1\mathbf{u} - \mathbf{F}_2\mathbf{v}$.

As stated in (SANTANA; BRANDÃO; SARCINELLI-FILHO, 2016), such a model is obviously not a complete description of rotorcraft dynamics. However, this formulation accurately describes the influence of high-level control signals on the vehicle's maneuvers.

From (4.7), v_x and v_y are the linear velocity along $x-$ and $y-$axis of the UAV body frame, whereas $\dot{z}$ and $\dot{\psi}$ are the linear and angular velocities along and around the z-axis, respectively, in the global frame. For experimental purposes, the Bebop's firmware provides the processed data readout of these variables.

Finally, $\mathbf{u} \in [-1, 1]$ is the normalized control signals. In summary, u_{v_x} and u_{v_y} represent pitch and roll commands, which indirectly causes a linear velocity and a dis-

placement along the x_B- and y_B-axis, respectively. In addition, $u_{\dot{z}}$ and $u_{\dot{\psi}}$ represent the inputs associated with $\dot{z}$ and $\dot{\psi}$, respectively.

In order to perform a positioning task, let us propose the control law

$$\mathbf{u} = \mathbf{F}_1^{-1}\left(\boldsymbol{\eta} + \mathbf{F}_2\mathbf{v}\right), \quad \text{with} \quad \boldsymbol{\eta} = \ddot{\mathbf{q}}_d + \mathbf{K}_d\dot{\tilde{\mathbf{q}}} + \mathbf{K}_p\tilde{\mathbf{q}}, \tag{4.8}$$

where $\tilde{\mathbf{q}} = \mathbf{q}_d - \mathbf{q}$ is the pose error, and $\mathbf{K}_d$ and $\mathbf{K}_p$ are positive defined gain matrices. Notice that this controller design follows the inverse dynamic formulation.

In order to demonstrate the system stability in the closed loop, let us take the following radially unlimited Lyapunov candidate function

$$V(\tilde{\mathbf{q}}, \dot{\tilde{\mathbf{q}}}) = \frac{1}{2}\tilde{\mathbf{q}}^\intercal\mathbf{K}_p\tilde{\mathbf{q}} + \frac{1}{2}\dot{\tilde{\mathbf{q}}}^\intercal\dot{\tilde{\mathbf{q}}} > 0. \tag{4.9}$$

By applying the first time derivative, and then replacing (4.7) and (4.8), we get

$$\begin{aligned}\dot{V}(\tilde{\mathbf{q}}, \dot{\tilde{\mathbf{q}}}) &= \tilde{\mathbf{q}}^\intercal\mathbf{K}_p\dot{\tilde{\mathbf{q}}} + \dot{\tilde{\mathbf{q}}}^\intercal\left(\mathbf{F}_1\mathbf{u} - \mathbf{F}_2\mathbf{v}\right) \\ &= \tilde{\mathbf{q}}^\intercal\mathbf{K}_p\dot{\tilde{\mathbf{q}}} + \dot{\tilde{\mathbf{q}}}^\intercal\left(-\mathbf{K}_d\dot{\tilde{\mathbf{q}}} - \mathbf{K}_p\tilde{\mathbf{q}}\right) \\ &= -\dot{\tilde{\mathbf{q}}}^\intercal\mathbf{K}_d\dot{\tilde{\mathbf{q}}} \leq 0.\end{aligned} \tag{4.10}$$

From the Lyapunov theory, we can conclude that $\dot{\tilde{\mathbf{q}}} \to 0$ for $t \to \infty$. Furthermore, $\dot{\tilde{\mathbf{q}}}$ and $\tilde{\mathbf{q}}$ are ultimately bounded. Finally, after applying the theorem of La Salle, we can also conclude that the unique invariant set in the closed-loop system is the equilibrium $[\tilde{\mathbf{q}}\ \dot{\tilde{\mathbf{q}}}]^\intercal = [\mathbf{0}\ \mathbf{0}]^\intercal$, which means also $\tilde{\mathbf{q}} \to 0$ for $t \to \infty$. Therefore, the regulation (or tracking) system is asymptotically stable.

4.4 Results and Discussion

4.4.1 Experimental Setup

This section describes the strategy used to evaluate the UAV-UGV cooperation in face of ground obstacles for the accomplishment of a load transportation task our configuration setup is show in Figure 23. As can be seen in the figure, the UGVs adopted are the Pioneer 3-DX nonholonomic unicycle mobile platform, and the UAV is the Bebop 2 quadrotor. The posture of the vehicles is tracked by the OptiTrack motion tracking system, consisting of 15 cameras, which are placed around the experimental arena. The data captured by using mocap technology is then used as a constraint to reduce the ambiguity of the real-time inverse kinematic process by capturing the posture of all elements that make up the experiment and thus updating the control signals. To communicate with the robots, the robot operating system (ROS) is used. As for the high-level control code, it

was executed by using MATLAB©. Communication between ROS and MATLAB is done through a proprietary MATLAB library, which emulates the necessary ROS nodes and topics. The positions of the load, the electromagnet, and the trailer are also captured by the OptiTrack system.

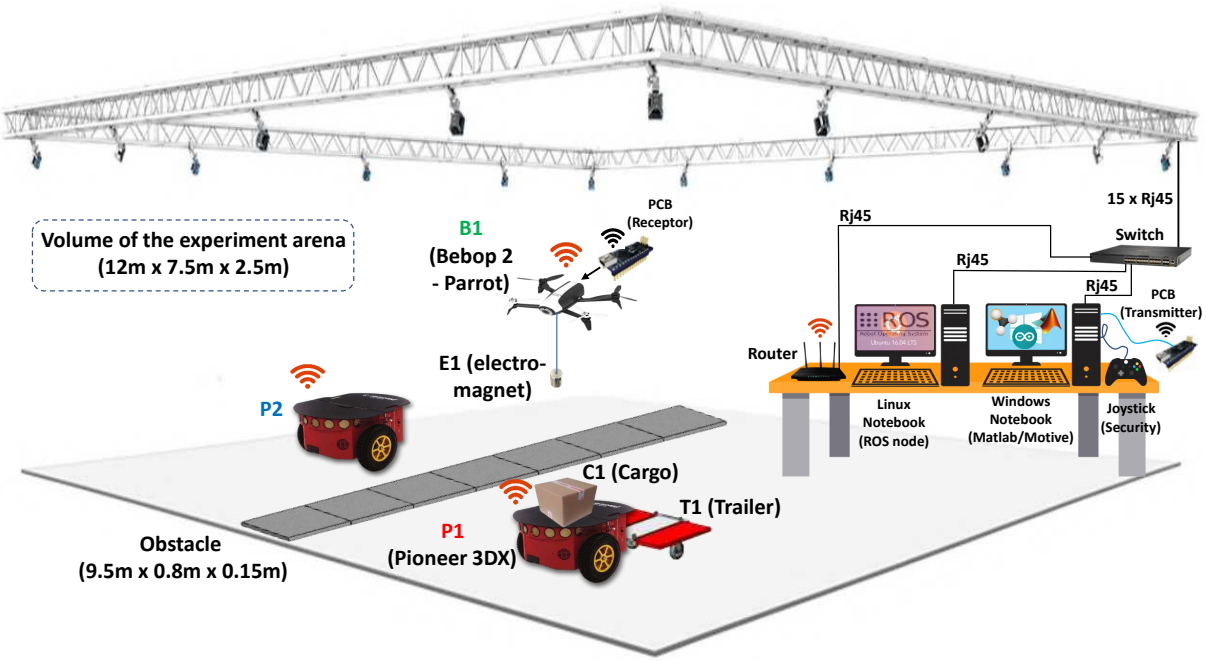

Figure 23 – The experimental setup to validate an experimental test as a proof of concept.

Once this work aims to perform a load transportation task, the electromagnet actuator is one of the main components of our system. However, the device should not have a permanent magnet, because the proposal considers capture and release actions only at opportune moments. Furthermore, to reduce the weight of the device, which must be on board the UAV, we have chosen to trigger it remotely. Thus, the capture and release action is decided externally and transmitted via wireless to the actuator.

The electromagnet has a capacity of up to 2.5 kg and runs on DC power through a two-cell, 7.4-V, 300-mA lithium polymer battery. The receiver board that controls the operation of the electromagnet is controlled by an Arduino Nano microcontroller. Furthermore, such a board allocates all the necessary components on a compact-sized board, so as not to interfere with the controllability of the UAV during flight. Table 1 lists the components used to make the transmitter and receiver, shown in Figure 24. Note that there is a yellow LED in Figure 24a. If it is on, the electromagnet is on; otherwise, it is off.

Importantly, one of the biggest challenges faced with suspended cable transportation is the effect of the load swinging after being captured by the electromagnet device. In other words, the actuator must be able to support the weight of the load even when the swing effect is present as a consequence of the UAV's displacement maneuvers. In the

Table 1 – Table of components used in transmitter and receptor.

Component	**Quantity**	**Present in Transmitter (T) or Receptor (R)**
Arduino Nano	2	T and R
Battery	1	R
TBJ 538	1	R
Electromagnet	1	R
LED	1	T
Push Button	1	T
Resistors 220 Ω	2	T and R
Switch	1	R
Radio NRF24L01	2	T and R
Antenna for WiFi Module	1	R
2.4 GHz Wireless Transceiver Module—NRF24L01	2	T and R

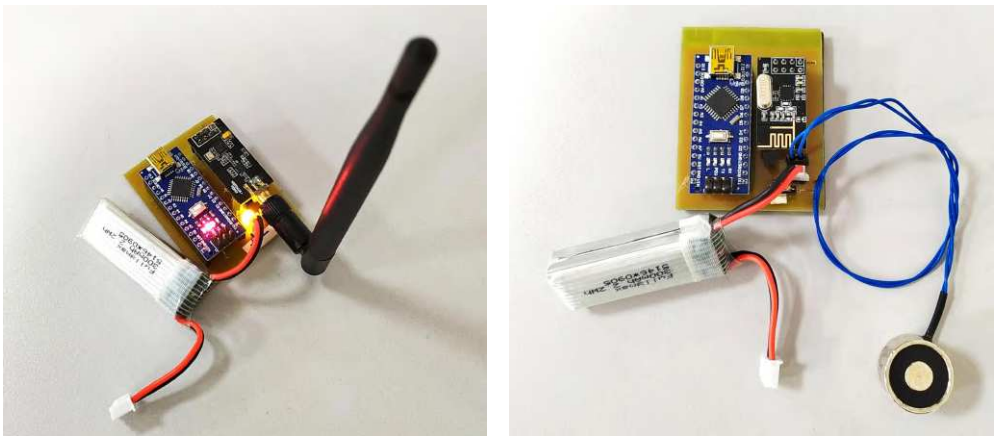

(a) Transmitter. (b) Receptor.

Figure 24 – Printed circuit boards (PCBs) for electromagnet actuation.

case of this work, cautious movements, with small angles of tilt and rotation of the UAV, helped mitigate the oscillations.

In terms of the load, it has a cubic shape of 10 cm side and weight of 72 g. Figure 25 shows two configurations: empty and full cargo. In the last case, a set of five styrofoam block increases the cargo weight by 25 g. The metal plate over the cargo prototype makes possible its interaction with the magnetic actuator.

4.4.2 Cooperative Task between UAV and UGVs

The following experiments examine the influence of the perturbation generated by the mass change during the holding and release action, and the ability of the system to

(a) Empty Cargo. (b) Full Cargo.

Figure 25 – Cargo transported in experiments.

handle it. For a better explanation, we divide our discussions into two subsections, wherein transport with loads of different weights are evaluated. In both cases, a heterogeneous formation with one UAV and two UGVs makes up the experiments.

4.4.2.1 Experiment #1

In the first experiment, the weight of the actuator and the payload is 90 g and 72 g, respectively, which corresponds to about 32% of the weight of the drone. The video presenting the entire experiment can be found at <https://youtu.be/0UIOjn5_a5s>. Table 2 presents in chronological sequence in which the robots perform each action cooperatively.

Experiment #1 is divided temporally into five regions: transportation, setup, lifting, returning, and transportation again. These regions make up the complete realization of the experiment. In addition, Figure 26 highlights the actions that B1 performs at each region transition: take off, docked, released and landing, respectively.

At the beginning of the experiment, only P1 starts its motion by carrying C1 and B1 through the T1 trailer. This step comprises the transportation region and occurs in the interval from 0 to 42 s. After 20 seconds, P1 reaches a previously defined desired point in an orientation perpendicular to the obstacle. At this instant, P2 comes from rest and starts moving to reach a position in front of P1 and also perpendicular to the obstacle.

Starting at 42 s, the setup region is initiated and occurs in the interval from 42 to 55 s. During this interval, B1 takes off, aiming to position itself under C1 in order to take it. The change in altitude of B1 in Figure 26 confirms such an action. Note also that before taking off, B1 is at a height close to 30 cm; after all this is the height of T1 added to the height of B1's center of gravity relative to T1.

In the interval from 52 to 55 s, it can be seen that E1 and C1 have the same vertical coordinate, i.e., the actuator is in contact with the load. This situation is maintained until the load is released.

Table 2 – Sequence of events of the experiment 1.

Seq	Time (mm:ss)	Region	Action	Snapshot (mm:ss)
1	00:01	Transportation	P1 carries (C1 + B1) to the combined point	01:25
2	00:22	Transportation	P1 arrives at the agreed point and triggers P2 which starts moving	01:47
3	00:42	Docked | Lifting	P2 reaches the combined point and triggers B1 to take off	02:07
4	00:55	Lifting	B1 picks up C1 using the electromagnet E1 and go to P2	02:20
5	01:08	Lifting | Returning	B1 releases C1 the under P2 and returns to the other side of the platform	02:33
6	01:18	Returning | Transportation	B1 positions himself above the trailer and lands	02:43
7	01:40	Transportation	The formation returns to their respective address and the task is successfully completed	02:50

Upon entering the lifting region, which occurs after 55 s, B1 grasps C1 and makes its transposition between P1 and P2, over the obstacle. It is worth remembering that P1 and P2 wait at rest until the transposition of the load is successfully completed. Notice in Figure 26 that the altitude of E1 and C1 are identical during this stage, which confirms that the payload is being lifted by the UAV. Note also that the distance between B1 and C1 represents the length of the suspended cable.

At the end of the lifting stage, note that C1 returns to the same altitude value that it had before being lifted from P1. This demonstrates that the load has been delivered to P2, and is confirmed by the change in the side elevation y, as seen in Figure 26.

At 67 s, B1 releases C1 over P2 and the returning region is initiated. After the delivery, B1 returns to land on T1. Finally, in the last region called transportation, which starts at 78 s, the entire formation moves to its destination point, successfully completing the entire transport task.

Note that the altitude variation observed in Figure 26, around 80 s, indicates B1's attempts to land on T1 and to have succeeded on the second attempt. It generally depends on how aligned B1 is with respect to T1.

4.4.2.2 Experiment #2

In the second experiment, the weight of the load is increased to 97 g. Consequently, the total weight to be lifted corresponds to about 37% of the weight of the UAV. The additional 25 g are used to evaluate the controller response under the same conditions of Experiment #1. The whole evaluation can be seen at <https://youtu.be/0UIOjn5_a5s>.

Table 3 presents the instants of the events of each action referring to Experiment #2. All the analysis and discussion of Experiment #1 also apply to Experiment #2. Notice that this time the landing of B1 on T1, after the delivery of C1, occurred on the first attempt. This can be seen in the altitude variable of B1 around 80 s in Figure 27.

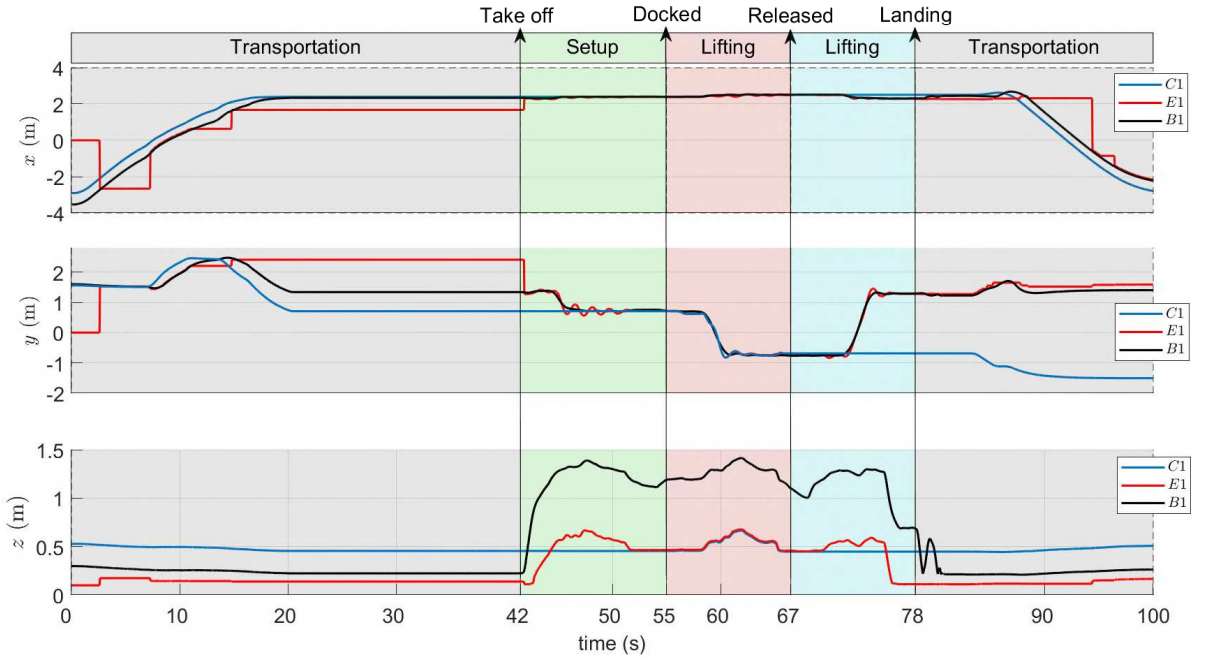

Figure 26 – Results of Experiment #1. Position time evolution of the cargo (C1), the electromagnet effector (E1), and the Bebop UAV (B1).

Comparatively, during the transport stage, the load showed greater longitudinal and lateral oscillations in Experiment #2 than in #1. This is a consequence of the additional mass of the load causing the oscillation amplitude to increase. However, the controller proved to be able to handle this disturbance.

Table 3 – Sequence of events of the experiment 2.

Seq	Time (mm:ss)	Region	Action	Snapshot (mm:ss)
1	00:01	Transportation	P1 carries (C1 + B1) to the combined point	03:15
2	00:22	Transportation	P1 arrives at the agreed point and triggers P2 which starts moving	03:33
3	00:42	Docked | Lifting	P2 reaches the combined point and triggers B1 to take off	03:53
4	00:55	Lifting	B1 picks up C1 using the electromagnet E1 and goes to P2	04:07
5	01:08	Lifting | Returning	B1 releases C1 under P2 and returns to the other side of the platform	04:21
6	01:18	Returning | Transportation	B1 positions himself above the trailer and lands	04:30
7	01:40	Transportation	The formation returns to their respective address and the task is successfully completed	04:34

Both experiments showed that it is possible to successfully coordinate a heterogeneous squadron to together perform a cargo transport mission, with the possibility of the UAV taking off and landing on a trailer connected to one of the UGVs. Furthermore, this work showed the application of an electromagnetic actuator connected to an overhead cable as an option to grab and release the cargo at the opportune moments of the transport mission. Finally, being an applied science project, the results demonstrated the stability of the controllers proposed in previous works, as well as their tolerance to the rejection of disturbances caused by load transportation.

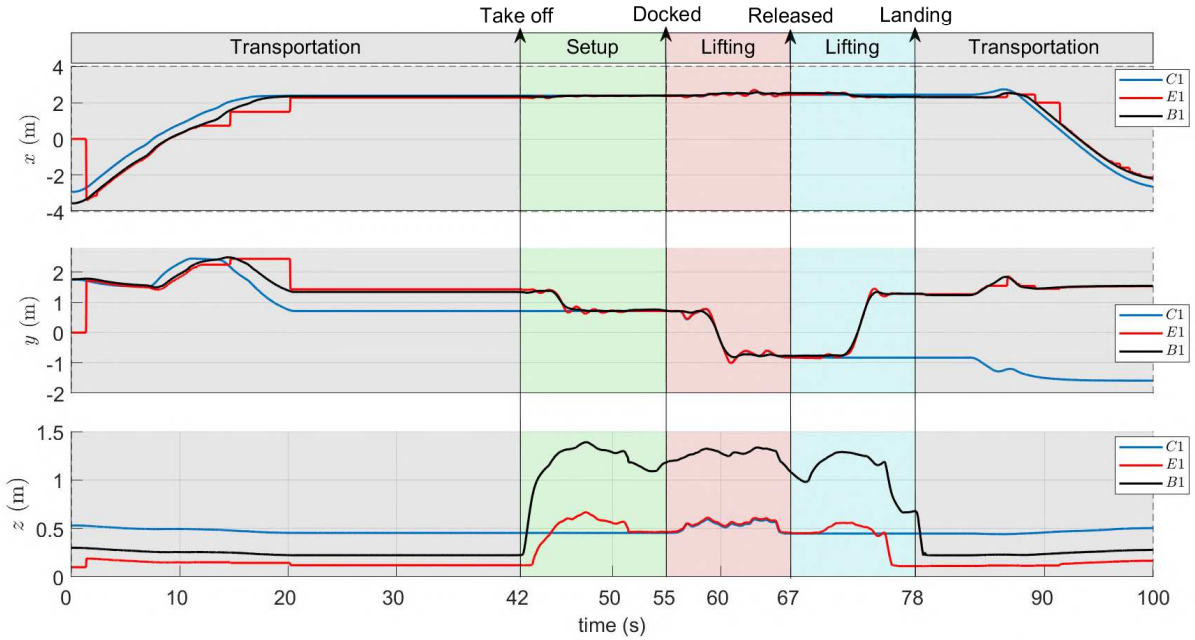

Figure 27 – Results of Experiment #2. Position time evolution of the cargo (C1), the electromagnet effector (E1), and the Bebop UAV (B1).

4.5 Concluding Remarks

This paper has presented a practical application of a heterogeneous formation of robots in performing a task of lifting, transporting, and delivering cargo by suspended cables. The problem addressed was the impossibility of transporting a load by using only ground robots, due to the presence of an obstacle that prevented its transposition. Therefore, a UAV capable of flying was in charge of transporting the load over the obstacle and delivering it to the destination robot.

The control strategies proposed in our previous work were used here to guide the vehicles. For the ground robots, the controller guided the vehicles to the meeting and destination points as planned. Notably, the way-points contributed to the robot-trailer set during its backward maneuvers. On the other hand, for the aerial robot, the controller proved to be capable of controlling the UAV, even in the presence of a load beyond its own weight. During navigation with lighter or heavier loads, small oscillations were observed in the lateral and longitudinal movements, but nothing that would compromise the stability of the set or even the accomplishment of the mission.

Finally, the electromagnetic effector developed proved to be a simple, economical, and efficient solution to perform cargo transport tasks. Although its load capacity is 2.5 kg, the lifting or dragging of such a mass could not be tested due to the load capacity of the UAV used. Thus, transporting heavier loads in more varied ways remains as an idea for future work.

5 Concluding Remarks

This chapter summarizes the key contributions of this dissertation, discusses the main challenges encountered throughout the research, and outlines potential directions for future work.

5.1 Contributions and Achievements

The primary objective of this dissertation was to enhance the efficiency, precision, and sustainability of UAV-based cargo transportation and aerial spraying by integrating real-time payload monitoring, vision-based control, and cooperative multi-agent strategies. To address this objective, the research was structured around key hypotheses, each validated through experimental studies. The main contributions of this work include:

- Development of a real-time payload weight sensor for UAVs, enabling precise control adjustments and improving resource efficiency in spraying and transportation tasks.
- Integration of the payload sensor into an adaptive spraying system, allowing dynamic pesticide application based on real-time weight variations, reducing chemical waste and optimizing agricultural treatment.
- Implementation of a vision-based control approach for UAV spraying, identifying target areas and optimizing pesticide distribution.
- Generation of optimized trajectories for spraying applications, allowing adjustments to acceleration signals and speeds in specific regions of the path.
- Development of cooperative UAV-UGV transportation strategies, enhancing operational efficiency by leveraging UAV agility for aerial transport and UGV stability for ground-based delivery.
- Experimental validation of control strategies for gripping or releasing the load via magnetic coupling in suspended load transportation tasks.

Each of these contributions aligns with the dissertation hypotheses, demonstrating the effectiveness of real-time sensing, adaptive control, and cooperative robotics in UAV-based logistics. The system's progressive evolution throughout the research was critical to its validation in diverse operational scenarios. While initial sensor-based approaches provided essential real-time data, integrating vision-based classification further enhanced decision-making autonomy, allowing UAVs to operate in dynamic environments without relying on external motion capture systems.

5.2 Limitations and Challenges

Despite the promising results, some limitations were identified during the research:

- The payload weight sensor, while effective in improving control accuracy, still presents challenges in adapting to sudden weight shifts, particularly in variable-mass liquid cargo.
- The vision-based spraying system, although capable of detecting target areas, is subject to environmental constraints such as lighting variations and occlusions, which may impact detection reliability.
- Cooperative UAV-UGV strategies require precise synchronization to ensure effective cargo transfer, and further optimization is needed to enhance communication and coordination between robotic agents.
- Stabilization of suspended loads remains a critical challenge, requiring further advancements in real-time control algorithms to mitigate pendular oscillations in dynamic flight conditions.
- Experimental validation of control strategies to mitigate oscillations in suspended load transport, ensuring greater stability and precision in cargo handling.

These challenges highlight the need for continued research to improve system robustness, particularly in adapting to complex real-world conditions and ensuring reliability across diverse operational scenarios.

5.3 Final Considerations

This dissertation explored key advancements in UAV-based transportation and aerial spraying, integrating real-time sensing, vision-based optimization, and cooperative robotics to enhance efficiency and precision. The findings validate the research hypotheses, demonstrating that adaptive control strategies and collaborative UAV-UGV approaches significantly improve UAV performance in logistics and agriculture.

Despite its limitations, the proposed system represents a step forward in making UAV applications more autonomous, efficient, and adaptable to real-world constraints. Future research should focus on refining sensor accuracy, improving the robustness of vision-based detection in varying environmental conditions, and optimizing cooperative control strategies for heterogeneous robotic teams. Additionally, further exploration of autonomous refueling mechanisms, multi-agent coordination strategies, and advanced AI-based perception techniques could significantly expand the applicability of UAV-assisted operations in industrial and agricultural contexts.

Bibliography

ALVES, W. F. d. O.; BARCELOS, C. O.; BRANDAO, A. S. A gesture recognition system for robot guidance applications. In: **Congresso Brasileiro de Automática-CBA**. Rio de Janeiro, Brazil: Sociedade Brasileira de Automática (SBA), 2024. v. 4, n. 1.

BARCELOS, C. O. et al. Enhancing uav spraying efficiency through payload sensor integration. In: IEEE. **2024 Latin American Robotics Symposium (LARS)**. Arequipa, Peru, 2024. p. 1–6.

BARCELOS, C. O. et al. Integration of payload sensors to enhance uav-based spraying. **Drones**, MDPI, v. 8, n. 9, p. 490, 2024.

BARCELOS, C. O. et al. Robot formation performing a collaborative load transport and delivery task by using lifting electromagnets. **Applied Sciences**, MDPI, v. 13, n. 2, p. 822, 2023.

BRANDÃO, A. S.; SARCINELLI-FILHO, M.; CARELLI, R. An analytical approach to avoid obstacles in mobile robot navigation. **International Journal of Advanced Robotic Systems**, SAGE Publications Sage UK: London, England, v. 10, n. 6, p. 278, 2013.

BRANDÃO, A. S. et al. Side-pull maneuver: a novel control strategy for dragging a cable-tethered load of unknown weight using a uav. **IEEE Robotics and Automation Letters**, IEEE, v. 7, n. 4, p. 9159–9166, 2022.

CARDONA, G.; TELLEZ-CASTRO, D.; MOJICA-NAVA, E. Cooperative transportation of a cable-suspended load by multiple quadrotors. **IFAC-PapersOnLine**, Elsevier, v. 52, n. 20, p. 145–150, 2019.

CHEN, H. et al. Aerial grasping with a lightweight manipulator based on multi-objective optimization and visual compensation. **Sensors**, MDPI, v. 19, n. 19, p. 4253, 2019.

ESTEVEZ, J. et al. A hybrid control approach for the swing free transportation of a double pendulum with a quadrotor. **Applied Sciences**, MDPI, v. 11, n. 12, p. 5487, 2021.

FAGUNDES-JUNIOR, L. A. et al. Bdp-uaifly system: A platform for the robocup brazil open flying robot trial league. In: IEEE. **2023 International Conference on Unmanned Aircraft Systems (ICUAS)**. Warsaw, Poland, 2023. p. 1021–1028.

FAGUNDES-JÚNIOR, L. A. et al. Uav–ugv formation for delivery missions: A practical case study. **Drones**, MDPI AG, v. 9, n. 1, p. 48, 2025.

FAGUNDES-JUNIOR, L. A. et al. Exploring the science and art of uav light painting: From equations and pixels to long-exposure photography. In: IEEE. **2024 International Conference on Unmanned Aircraft Systems (ICUAS)**. Chania - Crete, Greece, 2024. p. 755–762.

FIAZ, U. A.; TOUMI, N.; SHAMMA, J. S. Passive aerial grasping of ferrous objects. **IFAC-PapersOnLine**, Elsevier, v. 50, n. 1, p. 10299–10304, 2017.

GUERRERO, M. E. et al. Passivity based control for a quadrotor uav transporting a cable-suspended payload with minimum swing. In: IEEE. **2015 54th IEEE Conference on Decision and Control (CDC)**. Osaka, Japan, 2015. p. 6718–6723.

HUANG, J. et al. Suppressing uav payload swing with time-varying cable length through nonlinear coupling. **Mechanical Systems and Signal Processing**, Elsevier, v. 185, p. 109790, 2023.

JIMÉNEZ-CANO, A. et al. Precise cable-suspended pick-and-place with an aerial multi-robot system. **Journal of Intelligent & Robotic Systems**, Springer, v. 105, n. 3, p. 1–13, 2022.

KOTARU, P.; WU, G.; SREENATH, K. Differential-flatness and control of quadrotor (s) with a payload suspended through flexible cable (s). In: IEEE. **2018 Indian Control Conference (ICC)**. Kanpur, India, 2018. p. 352–357.

KREMER, P. et al. Trigger: A lightweight universal jamming gripper for aerial grasping. **IEEE Access**, IEEE, v. 11, p. 50098–50115, 2023.

LEMARDELÉ, C. et al. Potentialities of drones and ground autonomous delivery devices for last-mile logistics. **Transportation Research Part E: Logistics and Transportation Review**, Elsevier, v. 149, p. 102325, 2021.

LI, G.; GE, R.; LOIANNO, G. Cooperative transportation of cable suspended payloads with mavs using monocular vision and inertial sensing. **IEEE Robotics and Automation Letters**, IEEE, v. 6, n. 3, p. 5316–5323, 2021.

LOPEZ, M.; MARTINEZ-CARRANZA, J. A cnn-based approach for cable-suspended load lifting with an autonomous mav. **Journal of Intelligent & Robotic Systems**, Springer, v. 105, n. 2, p. 1–12, 2022.

MOGILI, U. R.; DEEPAK, B. Review on application of drone systems in precision agriculture. **Procedia computer science**, Elsevier, v. 133, p. 502–509, 2018.

PINTO, A. O. et al. High-level modeling and control of the bebop 2 micro aerial vehicle. In: IEEE. **2020 International Conference on Unmanned Aircraft Systems (ICUAS)**. Athens, Greece, 2020. p. 939–947.

PIZETTA, I. H. B.; BRANDAO, A. S.; SARCINELLI-FILHO, M. A hardware-in-the-loop platform for rotary-wing unmanned aerial vehicles. **Journal of Intelligent & Robotic Systems**, Springer, v. 84, p. 725–743, 2016.

REZENDE, F. d. A. et al. Gesture-based teleoperation assisting load transportation tasks. In: **Congresso Brasileiro de Automática-CBA**. Rio de Janeiro, Brazil: Sociedade Brasileira de Automática (SBA), 2024. v. 4, n. 1.

SANTANA, L. V.; BRANDÃO, A. S.; SARCINELLI-FILHO, M. Navigation and cooperative control using the ar. drone quadrotor. **Journal of Intelligent & Robotic Systems**, Springer, v. 84, p. 327–350, 2016.

SARKISOV, Y. S. et al. Development of sam: cable-suspended aerial manipulator. In: IEEE. **2019 International Conference on Robotics and Automation (ICRA)**. Montreal, QC, Canada, 2019. p. 5323–5329.

TANG, S.; WÜEST, V.; KUMAR, V. Aggressive flight with suspended payloads using vision-based control. **IEEE Robotics and Automation Letters**, IEEE, v. 3, n. 2, p. 1152–1159, 2018.

UBELLACKER, S. et al. High-speed aerial grasping using a soft drone with onboard perception. **npj Robotics**, Nature Publishing Group UK London, v. 2, n. 1, p. 5, 2024.

VILLA, D. K.; BRANDAO, A. S.; SARCINELLI-FILHO, M. A survey on load transportation using multirotor uavs. **Journal of Intelligent & Robotic Systems**, Springer, v. 98, n. 2, p. 267–296, 2020.

Appendix

APPENDIX A – Additional Contributions: Side Projects

Throughout the course of this research, several collaborative projects were developed in cooperation with other researchers from the Núcleo de Especialização em Robótica (NERo). These side projects contributed significantly to the development of novel UAV control, navigation, and perception strategies, reinforcing the core findings of this dissertation. Each study tackled different aspects of UAV automation and interaction, ultimately enriching the scope of autonomous aerial robotics.

A.1 BDP-UaiFly System: A Platform for the RoboCup Brazil Open Flying Robot Trial League

One of the projects developed was the BDP-UaiFly System, published in the *2023 Latin American Robotics Symposium (LARS)* (FAGUNDES-JUNIOR et al., 2023). This project focused on the application of autonomous UAVs in the *Flying Robot Trial League* (FRTL), a competition organized by RoboCup Brazil to foster the development of aerial robotics for industrial applications. The research introduced the navigation and perception system implemented by the BDP-Fly robotics team during the 2022 competition, utilizing the Parrot Bebop 2 UAV to execute equipment transportation tasks.

The primary objective of this project was to develop an integrated navigation and sensing platform that combined autonomous control strategies with computer vision techniques. The implementation of vision-based control mechanisms enhanced the UAV's ability to perform precise maneuvering, particularly for load transportation tasks. The experimental validation conducted throughout the competition demonstrated the feasibility of applying UAVs in industrial environments, such as pipeline inspection and automated logistics, where precise aerial control is critical.

The main contributions of this research include the development of an integrated navigation and sensing system that combines autonomous control with image processing techniques, the implementation of vision-based control for cargo transportation using the UAV's onboard camera for guidance, and the experimental validation of the system's stability and efficiency in real-world transportation missions.

The impact of this study extends beyond its immediate application in the RoboCup competition. The knowledge gained regarding image-processing-based control (PDI) was later applied to improve UAV navigation and spraying techniques in the dissertation's

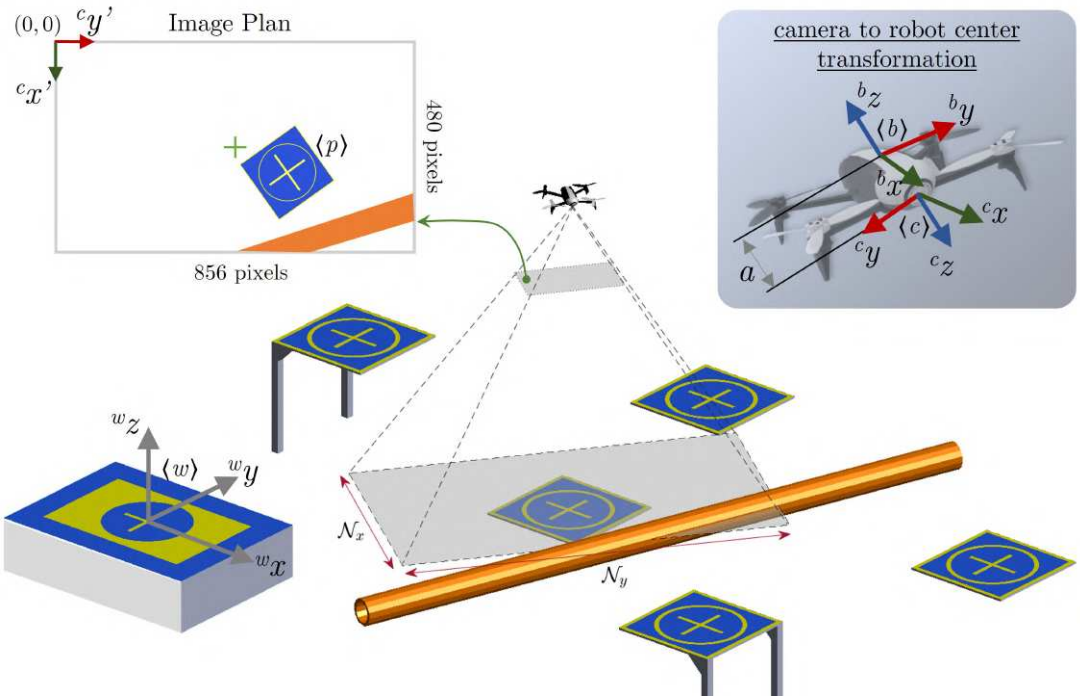

Figure 28 – Image processing for color pattern recognition suggested in (FAGUNDES-JUNIOR et al., 2023).

primary research. Additionally, the experience acquired in the development of this system provided a foundational understanding of sensor integration and control strategy calibration in agricultural UAV applications.

A.2 UAV–UGV Formation for Delivery Missions

The study (FAGUNDES-JÚNIOR et al., 2025) explored the concept of collaborative cargo transportation through a heterogeneous robotic formation, integrating two unmanned ground vehicles (UGVs) and an unmanned aerial vehicle (UAV). The research addressed a scenario in which an obstacle prevented direct interaction between the two UGVs, requiring the UAV to act as an intermediary in the delivery process. To achieve this, the UAV utilized a suspended electromagnet to lift and transport the cargo from one UGV to another, demonstrating an efficient aerial-ground logistics approach.

The primary objectives of this work were to develop a cooperative UAV-UGV system for cargo transportation, implement a physical coupling mechanism in which the UAV autonomously captured and delivered the cargo using an electromagnet, and experimentally validate the feasibility of the method with payloads representing up to 36% of the UAV's total mass. The results confirmed the effectiveness of the proposed approach, highlighting the potential of multi-robot collaboration for logistics applications.

The impact of this study extends to multiple areas of robotic logistics and transportation. The challenges addressed, such as precise suspended load control and real-time

interaction between distinct robotic platforms, contributed significantly to the development of this dissertation. Additionally, the insights gained from this research played a crucial role in refining control strategies for suspended cargo transportation, proposed in (BARCELOS et al., 2023).

A.3 Exploring the Science and Art of UAV Light Painting: From Equations and Pixels to Long-Exposure Photography

The use of UAVs for entertainment applications, such as *drone light shows*, has grown exponentially in recent years. This study explored a creative application of UAVs in visual arts, specifically in long-exposure photography (FAGUNDES-JUNIOR et al., 2024). The research presented in developed a trajectory control system based on optimization algorithms, allowing the UAV to follow parametric curves or digital image contours to create luminous patterns in the sky.

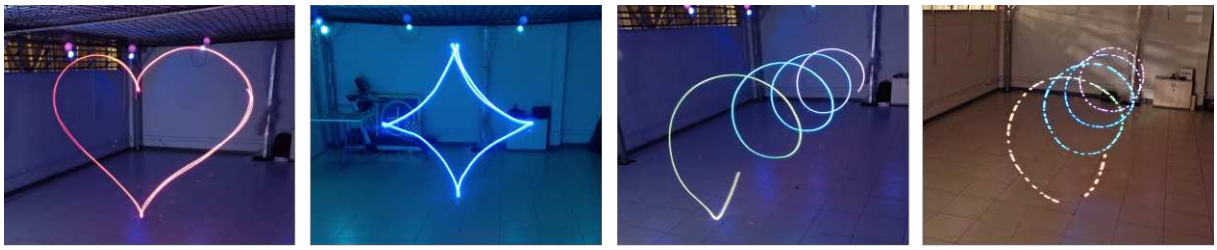

(a) (b) (c) (d)

Figure 29 – Light Painting photographs. (a) heart-shape, (b) astroid, (c)–(d) helical shape with color map and continuous and blinking LED states, respectively.

The main contributions of this work include the implementation of a trajectory planning system based on image recognition, which converts image edges into UAV flight paths, the development of an optimization method for waypoint generation to ensure smooth and safe trajectories within the UAV's workspace, and the experimental validation of the system through light painting techniques, demonstrating the precision of the generated flight paths.

The impact of this research goes beyond artistic applications. The control and trajectory planning techniques developed in this study were fundamental to optimizing flight trajectories for agricultural spraying applications in the dissertation. The ability to extract contours from images and convert them into precise flight commands was applied directly to the UAV's spraying system, allowing the drone to follow predefined application patterns with high precision. This approach contributed to improving the efficiency and precision of UAV-based agricultural operations, reducing wasted resources and optimizing the distribution of chemicals.

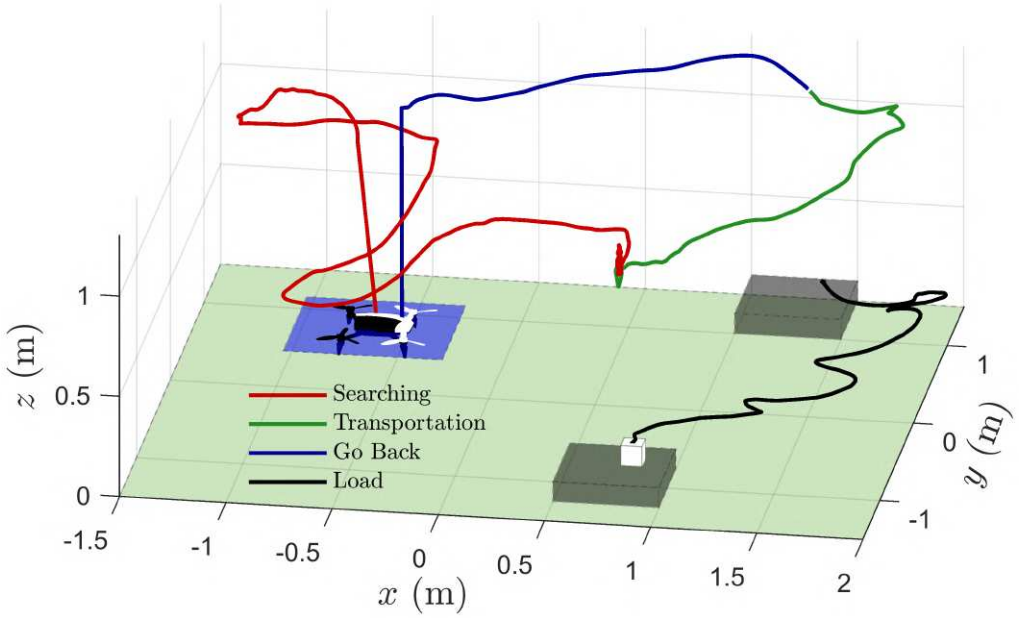

Figure 30 – UAV navigation by teleoperated control.

A.4 Gesture-Based Teleoperation for Load Transportation Tasks

The study (REZENDE et al., 2024) investigated the use of human gestures as an interface for UAV control in cargo transportation tasks. The proposed approach utilized reflective markers placed on the operator's hands, which were tracked by a motion capture system (OptiTrack Motive®). The motion data was processed in Matlab®, allowing the conversion of gestures into commands for controlling the Parrot Bebop 2 UAV.

The main contributions of this work include the development of a contactless and intuitive interface for UAV control in cargo operations, the implementation of a motion tracking system to detect and interpret human gestures, and the integration of the control system with the UAV, enabling the operator to manage cargo transportation and delivery tasks solely through gestures.

This study extends to the field of human-robot interaction, offering new possibilities for UAV control in logistics and agricultural missions. Additionally, this research contributed to refining supervised control methods, where an operator can intervene in UAV flight operations without the need for traditional physical control devices.

A.5 A Gesture Recognition System for Guidance Applications

The study (ALVES; BARCELOS; BRANDAO, 2024) focused on the development of a gesture recognition system (see Figure 31) for controlling autonomous robots, utilizing the Intel RealSense D435 camera and the K-Nearest Neighbors (KNN) algorithm. The research evaluated the accuracy of the method and its applicability in inspection and

teleoperation tasks.

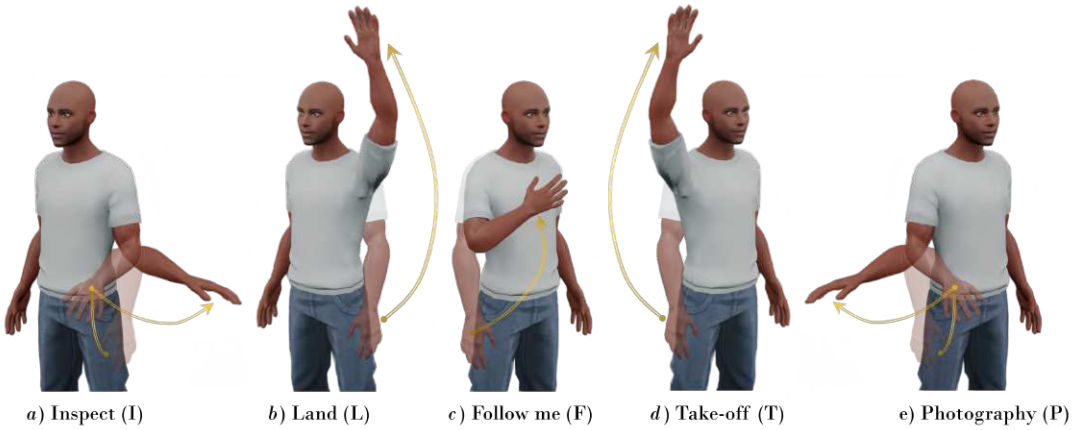

Figure 31 – Gesture patterns used for pattern recognition.

The main contributions include the implementation of a robust gesture recognition system achieving 94% accuracy in command classification, application in remote inspection tasks allowing intuitive UAV control, and the study of teleoperation-assisted navigation by integrating gesture recognition with autonomous navigation strategies.

This research contributed to the dissertation by offering an alternative approach for UAV control, exploring the integration of natural interfaces for drone command. The methodology developed can be applied to the supervision of agricultural missions or intuitive interaction between operators and UAVs in industrial settings.